Published in final edited form as:

J Immunol. 2019 October 15; 203(8): 2194–2209. doi:10.4049/jimmunol.1900230.

Mycobacterium tuberculosis-induced BAL gene expression signature in latent tuberculosis infection is dominated by pleiotropic effects of CD4+ T cell-dependent IFNγ production despite the presence of polyfunctional T cells within the airways

Jessica Jarvela, M.S.[1,3], **Michelle Moyer, M.S.**[1,3], **Patrick Leahy, Ph.D.**[4], **Tracey Bonfield, Ph.D**[5], **David Fletcher, B.S.**[5], **Wambura N. Mkono, M.D.**[1,2,3], **Htin Aung, M.D.**[6,7], **David H. Canaday, M.D.**[6,7], **Jean-Eudes Dazard, Ph.D.**[8], **Richard F. Silver, M.D.**[1,2,3,*]

[1]Division of Pulmonary, Critical Care and Sleep Medicine, Louis Stokes Cleveland Department of Veteran's Affairs Medical Center, Cleveland OH, USA

[2]Division of Pulmonary, Critical Care and Sleep Medicine, University Hospitals Cleveland Medical Center, Cleveland OH, USA

[3]Division of Pulmonary, Critical Care and Sleep Medicine, Case Western Reserve University School of Medicine, Cleveland OH, USA

[4]CWRU Comprehensive Cancer Center, Case Western Reserve University School of Medicine

[5]Division of Pediatric Pulmonology, Allergy, and Immunology, Case Western Reserve University School of Medicine

[6]Division of Infectious Diseases and HIV Medicine, Louis Stokes Cleveland Department of Veteran's Affairs Medical Center

[7]Division of Infectious Diseases and HIV Medicine, Case Western Reserve University School of Medicine

[8]Center for Proteomics and Bioinfomatics, Case Western Reserve University School of Medicine

Abstract

Tuberculosis (TB) remains a world-wide public health threat. Development of a more effective vaccination strategy to prevent pulmonary TB, the most common and contagious form of the disease, is a research priority for international TB control. A key to reaching this goal is improved understanding of the mechanisms of local immunity to *Mycobacterium tuberculosis* (*Mtb*), the causative organism of TB. In this study, we evaluated global *Mtb*-induced gene expression in airway immune cells obtained by bronchoalveolar lavage (BAL) of individuals with latent tuberculosis infection (LTBI) and *Mtb*-naïve controls. In prior studies, we demonstrated that BAL cells from LTBI individuals display substantial enrichment for *Mtb*-responsive CD4+ T cells compared to matched peripheral blood samples. We therefore specifically assessed the impact of depletion of CD4+ and CD8+ T cells on *Mtb*-induced BAL cell gene expression in LTBI. Our

*Address correspondence to: Richard F. Silver, M.D., Division of Pulmonary, Critical Care and Sleep Medicine, Biomedical Research Building, Rm. 327, Case Western Reserve University School of Medicine, 10900 Euclid Avenue, Cleveland, OH 44106-4941, Phone: (216) 368-1151 Fax (216) 368-1142.

studies identified 12 canonical pathways and a 47-gene signature that was both sensitive and specific for the contribution of CD4+ T cells to local recall responses to *Mtb*. In contrast, depletion of CD8+ cells did not identify any genes that fit our strict criteria for inclusion in this signature. Although BAL CD4+ T cells in LTBI displayed polyfunctionality, the observed gene signature predominantly reflected the impact of IFNγ production on a wide range of host immune responses. These findings provide a standard for comparison of the efficacy of standard BCG vaccination as well as novel TB vaccines now in development at impacting the initial response to re-exposure to *Mtb* in the human lung.

INTRODUCTION

Tuberculosis (TB) remains a major threat to international public health, with recent estimates indicating that over 1.5 million individuals die each year from the disease [1]. *Mycobacterium tuberculosis (Mtb)* the causative organism of TB, is transmitted through the inhalation of infectious droplet particles, which, if they effectively evade non-specific host defenses, establish initial infection within the lungs. Most often, infected individuals develop antigen-specific immunity which serves to contain, but not fully eliminate viable *Mtb* organisms [2]. Current vaccination against *Mtb* uses the attenuated *M. bovis* strain BCG, which is typically administered via intradermal injection to newborns. Although BCG vaccination helps prevent the development of disseminated tuberculosis (TB) in very young children, it is not proven to prevent the development of active pulmonary TB, which is the most common, most contagious, and mostly deadly form of the disease [3–5]. Multiple candidate tuberculosis vaccines are currently in development [6], but their evaluation in human subjects is hampered by the lack of clear immunologic correlates of protection that may indicate which prospective vaccines are most promising for advancing into large-scale clinical trials [7–8]. However, multiple vaccine studies in animals have emphasized the importance of localization of immune responses to the lung in outcomes following subsequent respiratory *Mtb* exposure [9–12].

We have previously reported various assessments of local pulmonary immune responses in otherwise healthy individuals with latent tuberculosis infection (LTBI) who were not previously vaccinated with BCG [13–15]. These individuals represent a human population in whom the development of mycobacterial-specific immunity developed following natural respiratory infection with *Mtb*. We presumed that the immune responses of these individuals would demonstrate local enrichment for *Mtb*-responsive T cells within the lung and, indeed, we found that CD4+ T cells capable of IFNγgg production in response to stimulation with purified protein derivative of *Mtb* (PPD) were approximately 50-fold more frequent in cells from baseline bronchoalveolar lavage (BAL) in these individuals than in their peripheral blood. Further, localization of these memory cells to the lung allowed for rapid in vivo production of IFNγ-inducible chemokines capable of mediating recruitment of additional cells into the airways in response to bronchoscopic PPD challenge [14].

Prior studies have indicated the importance of early localization of antigen-specific CD4+ T cells to the lung in vaccine-induced immunity to *Mtb* [16–18]. Subsequent studies more specifically indicated a role for multi-functional CD4+ T-cells capable of producing IFNγ,

IL-2 and/or TNFα in optimizing immunity within the airways [19–21]. In addition, despite the key role of Th1-associated immunity in protecting against TB, other CD4+ T cell populations (notably Th17 cells) as well as CD8+ T cells have been implicated as contributing to protection as well [22–26]. These observations led us to undertake a more comprehensive approach to evaluating the impact of localized T-cell subsets in the recall responses of individuals with LTBI. We hypothesized that *Mtb*-responsive CD4+ T cells, while comprising less than 1% of all cells in baseline BAL of LTBI subjects, nevertheless have a dominant impact on global *Mtb*-induced gene expression of airway immune cells. Our studies involved *in vitro* infection of unsorted BAL cells from LTBI subjects, as well as BAL cells from which CD4+ or CD8+ T cells had been depleted, in microarray-based assessments of global *Mtb*-induced gene expression by immune cells from the first site of *Mtb* re-exposure, the airways. Our findings were compared to those observed in *Mtb* infection of BAL cells from *Mtb*-naïve control subjects. In making these assessments, we sought to identify a CD4+ T-cell dependent BAL cell gene expression signature of LTBI that may provide a basis for comparison with local airway immune responses induced using various immunization strategies. To clarify the potential contributions of various CD4+ T-cell cytokines to this signature, we also evaluated production of IFNγ, IL-2, TNFα, and IL-17 from supernatants of BAL cells cultured in medium alone or infected *in vitro* with *Mtb* for these gene-expression studies. In addition, we utilized intracellular cytokine staining for these same cytokines to evaluate the polyfunctionality of BAL CD4+ T cells in LTBI. Our findings provide a comprehensive evaluation of the ability of memory CD4+ T cells of the distal airways to contribute to initial recall responses to respiratory re-exposure to *Mtb*; they also provide a basis for comparison of these responses in recipients of standard ID vaccination with BCG as well as in individuals who are immunized via novel routes or with newly developed prospective TB vaccines.

MATERIALS AND METHODS

Subjects

Eligibility for research bronchoscopy was based on age 18–50, non-smoking status, and lack of other significant medical problems including asthma or other chronic respiratory disease, cardiac disease, or ongoing use of systemic immunosuppressive agents for any reason. LTBI subjects were self-identified on the basis of prior positive PPD skin test or QuantiFERON TB Gold In-Tube (QFN-GIT) blood test. Subjects with a history of BCG vaccination were excluded. Each subject underwent both skin-testing and QuantiFERON testing for study purposes. All 11 LTBI subjects had positive skin-test responses to PPD (using criteria of 10 mm or more of induration). Of these, 9 also had positive QuantiFERON testing. Given the lack of BCG vaccination in our cohort and the known frequency of discordant skin-test and IGRA results [27], subjects were not excluded based on negative QuantiFERON testing alone. No LTBI subjects had a prior history of active TB or of any symptoms suggestive of current disease, such as cough, night sweats, fevers, or weight loss. All underwent chest x-rays that showed no evidence for active TB. The status of *Mtb*-naïve control subjects was also confirmed by negative responses (0 mm induration) to PPD skin testing.

All protocols involving human subjects were approved by the Institutional Board of Review of Case Western Reserve University and University Hospitals Cleveland Medical Center and of the Louis Stokes Cleveland Department of Veterans' Affairs Medical Center.

Collection and processing of bronchoalveolar lavage (BAL) cells

All bronchoscopies were performed in the Dahms Clinical Research Unit (DCRU) at University Hospitals Cleveland Medical Center as previously described [14]. BAL samples were obtained by instillation and subsequent withdrawal of up to eight 30 mL aliquots of pre-warmed buffered saline. Recovered BAL fluid was placed on ice for transport to the laboratory. Samples were aliquoted into 50 ml polypropylene tubes and immediately centrifuged at 2000 RPM (480 x g) for 10 minutes. BAL cells were stained and counted using a hemocytometer.

Cell preparation

BAL cells were prepared for infection as unsorted samples, and following depletion of CD4+ or CD8+ T-cells. For T-cell subset depletion, BAL cells were incubated with magnetized EasySep antibodies (CD4 #18052, CD8 #18053 StemCell Technologies, Cambridge MA) and collected following passage through EasySep magnet using EasySep human cell depletion protocols. Following depletion, flow cytometry was used to confirm the efficacy of T-cell depletion; samples were not used in further studies unless removal of at least 90% of the targeted T-cell subset was achieved. Due to limitations of cell numbers and significant cell loss during depletion procedures, CD4+ and CD8+ T cells could not always be depleted in parallel from the same samples.

Infections

Following counting, unsorted and T-cell depleted BAL samples were resuspended in 4 ml of IMDM with 30% autologous serum (AS) and 1% penicillin G and aliquoted into sterile screw-topped microfuge tubes (Sarstedt, #72.692.005, Newton, NC) with at least 1e6 cells per tube. Frozen stocks of virulent *Mtb* strain H37Rv (#NR-123, BEIresources, Manassas VA) were thawed and prepared for infection by vortexing with sterile glass beads followed by centrifugation to remove clumped bacteria. After re-suspension in 30% autologous serum/IMDM/penicillin, infections were performed using a 3:1 bacteria-to-cell ratio as previously described [28]. For uninfected control samples, initial culture medium was replaced with 30% autologous serum/IMDM/penicillin alone. After 2 hours of incubation, microfuge tubes were centrifuged at 2000 RPM (480 x g). Supernatants were discarded (removing non-phagocytosed organisms from infected samples) and cell pellets were resuspended in 1 ml IMDM with 10% AS and 1% PCN. Cells were then incubated at 37°C in a 5% CO_2 incubator. Twenty-four hours later, all tubes were again centrifuged. Supernatants were removed and frozen for later use in assessing *Mtb*-induced cytokine production (below). Cell pellets were fast-frozen by placing microfuge tubes in dry ice for 5 minutes prior to transfer to −80 storage until use in RNA preparation.

Sample preparation and performance of microarrays

Batched frozen cell pellets were lysed with mirVana buffer (# AM1560, ThermoFisher Scientific, Waltham MA), mRNA isolated and cDNA synthesized according to mirVana protocols. Samples were run on Affymetrix Human Genome U133 plus 2.0 arrays (ThermoFisher Scientific)

Assessment of Mtb-induced BAL cell cytokine production

Cytokine concentrations if BAL culture supernatants were assessed using the Human Magnetic Luminex Assay reagents for simultaneous assessment of concentrations of IFNγ, IL-2, TNFα and IL-17 (R&D Systems, Minneapolis, MN). Standard curves for each cytokine (in duplicate) were generated by using the reference cytokine concentrations supplied in this kit. Samples were analyzed using the Luminex 100 IS Multiplex Bio-Assay Analyzer (Bio-Rad Laboratories, Hercules, CA). Statistical analysis of unsorted and T-cell depleted samples utilized paired t-tests as performed in Prism 7.0 (GraphPad Software, San Diego CA)

Assessment of BAL T-cell polyfunctionality

In separate experiments, BAL cells from individuals with LTBI were utilized in assays of cytokine production using intracellular cytokine staining. Cells were incubated with medium alone or purified protein derivative of *Mtb* (PPD, 10 μg/ml, Staten Serum Institut, Copenhagen, Denmark). After an initial 2-hr incubation at 37°C, 20 μg/ml Brefeldin A (#347688; BD Biosciences, San Diego CA) was added to each tube. All samples were then further incubated overnight at 37°C for a total of 24 h of stimulation.

The next morning, cells were incubated with live/dead aqua and with a surface staining antibody cocktail of CD14 Qdot 655, CD27 Qdot605, CD45RA PE-Texas red (ThermoFisher), CD3 PerCP, CD4 APC-Cy7 (Biolegend, San Diego CA) and CCR7 PE-Cy7 (BD Biosciences). Samples were then washed, fixed, and permeabilized with BD Cyotfix/ Cytoperm for ICS using IFNγ AF700, IL-2 APC, TNFα Pacific Blue, and IL-17 PE (Biolegend). Samples were again washed and resuspended in 1% paraformaldehyde for data acquisition on an LSR-II flow cytometer (BD Biosciences). Analysis was based on cytokine production by live CD4+ effector memory T cells (T_{EM}) based on lymphocyte gate singlets and gating on the CD14-, CD3+, CD4+, CD45RA-, CCR7- population using Boolean analysis of Flow Jo (Tree Star) and Simplified Presentation of Incredibly Complex Evaluations (SPICE, Mario Roederer, NIAID, Bethesda, MD) to assess polyfunctionality [29].

Statistical and functional analysis of gene expression data

Power analysis and sample size calculations—Power analyses and sample size calculations for microarray studies were based on controlling the False Discovery Rate (FDR) as previously described [30–35] and detailed in Supplemental Figure 1.

Pre-filtering, Normalization, Variance Stabilization and Correction for Normality—As detailed in Supplemental Figure 2, preprocessing issues upstream of the statistical analyses were addressed through the use of implementations and algorithms

available from the R project, a platform for statistical computing and visualization that is freely available to academic users through the the Comprehensive R Archive Network (CRAN) consortium (http://cran.r-project.org/). The dataset of measured intensities was corrected for global normalization, variance-stabilization and normality using our previously described *'Joint Adaptive Mean-Variance Regularizati*on' procedure [35] as implemented in our R package 'MVR' [36].

Bayesian ANOVA Differential Expression Analyses—Assessment of differential expression of mRNA probesets utilized a Bayesian hierarchical model and called "Bayesian ANOVA" as currently implemented as a R package 'spikeslab', and as a stand-alone Java-based software Bayesian Analysis of Microarray (BAM), freely available to academic users (www.bamarray.com), also detailed in Supplemental Figure 2 [37–42]. Further analysis was based on an absolute Z-cut value of 2.5 for each data set. Supplemental Figure 2 also includes M-shaped scatter plots of gene expression for each study group; these are comparable to volcano plots used to display probabilities in methods of p-value based methods of analysis.

Pathway and Network Analyses—All functional analysis of the interactions of differentially-expressed genes utilized Ingenuity Pathway Analysis software (https://www.qiagenbioinformatics.com/products/ingenuity-pathway-analysis/, QIAGEN Silicon Valley, Redwood City, CA, USA). For "Pathways Analysis", metabolic and signaling pathways were determined by first matching our lists of significantly up- or down-regulated genes (mRNA probesets) to unique HUGO gene symbols, then by comparing the abundance of these unique HUGO gene symbols with those in the 320 Ingenuity canonical metabolic and signaling pathways (as of Q4 2017). Ingenuity proprietary algorithms were used to build gene-gene interaction networks based on the connectivity of our lists of differentially expressed genes. The p-values of significant canonical pathways and networks were computed using right-tailed Fisher exact test probabilities and scores represented as the negative log of the calculated p-values. In this approach, only over-represented pathways and networks (i.e., those that have more molecules than expected by chance) are significant. Functional comparison analyses between our datasets were based on heatmaps of p-value statistics of the identified Canonical Pathways. To account for multiple hypothesis testing, multiple inference corrections were made using the Benjamini-Hochberg (B-H) method [30]. In this approach, B-H adjusted p-values represent an upper bound for the expected fraction of falsely rejected null hypotheses among all tests with p-values smaller than a certain level (usually $\alpha = 0.05$); the chosen p-value therefore corresponds directly to the rate of false positives findings calculated to be significant (i.e., the False Discovery Rate or *FDR*). Agreement between networks as assessed in the various study conditions was assessed using the Intraclass Correlation Coefficient (ICC) [43–45]. Here, the ICC and derived F-test p-values were derived to assess the consistency or agreement between any two experimental contrasts (*ICC ratings*) of observed Z-cuts values on genes/nodes (*ICC units*) in a given gene-interaction network/graph of an experimental contrast (*ICC group*).

RESULTS

BAL cell parameters of LTBI and Mtb naïve subjects

The basic BAL cell parameters for LTBI and *Mtb*-naïve subjects are compared in Table I. Consistent with previous reports [13, 46], no differences between the two groups were observed with regard to total BAL cell numbers or differential counts. Of specific interest for our subsequent depletion studies, there were no significant differences in the percentage of lymphocytes or in the CD4:CD8 T-cell ratios of BAL from LTBI and *Mtb*-naïve subjects.

Mtb-induced BAL cell gene expression in LTBI and Mtb-naïve controls

Due to limitations of cell numbers, it was not always possible to perform depletions of both CD4+ and CD8+ T-cells on each BAL sample. Accordingly, we did not have CD8 depletion data for all subjects in whom CD4+ T-cell depletion was performed; likewise, not all CD4+ and CD8+ T-cell depletion data was matched. Each dataset was therefore evaluated separately and compared independently to findings observed in BAL cells from *Mtb*-naïve subjects. The microarray data analyzed in this manuscript has been uploaded to the Gene Expression Omnibus repository (https://www.ncbi.nlm.nih.gov/geo/) and are listed as reference series GSE134566.

Lists of BAL cell genes found to be differentially expressed in response to *Mtb* infection are provided in Supplemental Table I. In studies of unsorted BAL samples from which paired CD4+ depleted samples were evaluated (n=11), *Mtb* infection resulted in significant changes in expression of 469 unique annotated genes (327 upregulated, 142 downregulated, Supplmental Table 1A). *Mtb*-induced gene expression in unsorted BAL cells from the studies that involved CD8 depletion yielded similar results, with significant changes being observed for 427 genes (235 upregulated, 192 downregulated, Supplemental Table 1B), whereas in *Mtb* naïve subjects (n=6), differential expression was observed for 287 genes (171 upregulated, 116 downregulated, Table Supplemental Table 1C)

Canonical pathways

Using IPA analysis of the gene lists noted above, canonical pathways associated with *Mtb* infection of unsorted BAL cells from LTBI individuals were evaluated. Using a stringent criteria of p-value <0.001 (ie, -log p>3), 51 canonical pathways were identified (Table II). The impact of CD4 T-cell depletion was expressed as the change in significance of identification of these pathways. Specifically, based on the criteria of change in p-value of > 2 logs, the significance of 34 of the 51 pathways (67%) was reduced in CD4-depleted samples. In terms of the general profile of CD4+ T cell function in these samples, it was notable that following CD4 depletion there was a marked decline in the significance of several pathways in which IFNγ plays a substantial role (“interferon signaling”, “crosstalk between dendritic cells and natural killer cells”, “Th1 pathway”, “Th1 and Th2 activation pathway, antigen presentation pathway”, “activation of IRF by cytosolic pattern recognition receptors”, “iNOS signaling”, “allograft rejection signaling”, and “role of JAK1, JAK2 and TYK2 in interferon signaling”, Figure 1A). In contrast, the threshold of a 2-log decline in p-value following CD4 depletion was not reached for any of several IL-17 associated pathways identified; to the contrary, the significance of three of these pathways (“role of IL17F in

inflammatory airway disease" and "role of IL17A signaling in fibroblasts" and "IL-17 signaling") actually increased following depletion (1B).

Expression of the 34 pathways in which the 2-log decline in significance was observed following CD4 depletion from LTBI BAL was then compared to that observed in the *Mtb*-induced gene expression responses of BAL cells from *Mtb*-naïve subjects (Figure 2A). For 12 of the 34 pathways for which CD4 depletion in LTBI subjects resulted in a decline in p-value of >2 logs following CD4 depletion in LTBI individuals, pathway p-values were also >2 logs lower in *Mtb*-naïve than LTBI subjects (Figure 2B). We therefore viewed these 12 pathways as being most significant for the impact of resident BAL CD4+ T cells in creating a unique signature of BAL cell immune memory to *Mtb*.

Parallel evaluation of studies involving depletion of CD8+ T cells from BAL of LTBI subjects revealed 6 pathways which fit both conditions of displaying a reduction of pathway p-value by > 2 logs following CD8 depletion as compared to unsorted BAL cells in LTBI, and a > 2 log difference between pathway expression in unsorted BAL cells of LTBI and *Mtb*-naïve control subjects. Of these 6 pathways, 4 were common to those impacted by CD4-depletion ("Allograft rejection signaling", "Antigen presentation pathway", "Crosstalk between dendritic cells and Natural Killer cells", and "Protein ubiquitination pathway"), whereas 2 were uniquely identified within the CD8 depletion studies ("Autoimmune thyroid disease signaling" and "T helper cell differentiation", data not shown).

Gene signatures

The twelve CD4-associated and six CD8-associated pathways identified by the criteria stated above were then scrutinized further in terms of specific genes for which in vitro *Mtb*-infection induced changes in gene expression in LTBI subjects. Again, we sought a specific pattern of genes for which i) expression was significant in unsorted BAL cells from LTBI individuals, ii) p-values were reduced by > 2 logs following CD4 depletion, and iii) p-values were also at least 2 logs lower in unsorted BAL cells of *Mtb*-naïve individuals than in those of LTBI subjects. Of 68 differentially-expressed genes in the CD4-associated pathways, a set of 47 genes fulfilled these criteria, as detailed in Table III. In contrast, none of the 31 genes identified in the CD8-associated pathways met these criteria (not shown). The 47 genes identified in Table III therefore comprise the CD4+ T-cell mediated signature of *Mtb*-induced gene expression in BAL cells of individuals with LTBI. A summary of the major functions of the products of the genes represented in this signature is provided in Supplemental Table S2. In addition to the anticipated inclusion of many genes involved in Th1-associated cell-mediated immunity, it was notable that 9 of the 47 genes of this signature (19%) are primarily characterized as being associated with anti-viral immune responses, of which several are noted specifically as components of immunity to influenza. Further, despite the IFNγ-dependence of many of the signature genes, they do not cluster into a limited number of processes, but rather reflect the pleiotropic impact of IFNγ, particularly on multiple aspects of host immunity.

Upstream regulators

Because limited BAL cell numbers prevented us from assessing *Mtb*-induced gene expression at multiple timepoints, we utilized IPA to review "upstream regulators" within the expression profiles observed within the varying conditions detailed above. Here we again made this assessment based on changes in the -log (adjusted p-value) in comparisons of unsorted BAL cells from LTBI subjects with those of T-cell depleted BAL in LTBI and unsorted BAL cells of *Mtb*-naïve subjects. In CD4 depletion studies, 75 upstream regulators identified within unsorted BAL cells in LTBI were found to be less significant by at least 2 logs in both CD4-depleted BAL cells of these same subjects and in unsorted BAL cells of *Mtb*-naïve subjects. Seventy-three upstream regulators were identified by these same criteria in studies of CD8 depletion. In both comparisons, upstream regulators associated with type I interferons were prominent; these accounted for 30 of the 75 identified regulators in CD4 depletion studies and 31 of 73 regulators identified in the CD8 depletion studies. As is consistent with the greater impact of CD4 depletion on overall *Mtb*-induced BAL cell gene expression, the change in p-values of these regulators was generally substantially greater with depletion of CD4+ T cells than CD8+ T cells (Figure 3). Of the non-type I IFN associated upstream regulators (as based on decrease in significance with T-cell depletion), greater diversity was observed between the impact of CD4 and CD8 depletion; however, the change in p-value associated with CD4 depletion remained markedly greater than that observed with CD8 depletion, as detailed in Table IV.

Clustering analysis

The 47 genes of the CD4+ T-cell mediated signature of *Mtb*-induced gene expression in BAL cells of individuals with LTBI were arranged by hierarchical clustering using the average or complete linkage method; the number of significant clusters (*K*) was determined by the Gap Statistic method [47]. In this method, the clustering is based on the patterns of gene expression observed within each sample and is blinded as to the study conditions represented by the samples. As illustrated in Figure 4, samples from both *Mtb*-naïve and LTBI subjects segregated into two gene expression clusters. For *Mtb*-naïve subjects, the clusters separated BAL gene expression from BAL samples incubated in medium alone from those in which cells had been infected with *Mtb*, with the exception of uninfected BAL cells from one subject which clustered with the *Mtb*-infected samples (4A). Samples from BAL cells of LTBI subjects represented three study conditions (unsorted cells maintained in medium alone and both unsorted and CD4-depleted cells that were infected in vitro with *Mtb*). Nevertheless, LTBI samples also segregated into only two clusters, with uninfected BAL and CD4-depleted *Mtb*-infected cells largely clustering together into one group. Of 11 samples from each condition, only 1 sample of uninfected BAL cells and one CD4-depleted, *Mtb* infected sample clustered with the unsorted *Mtb*-infected BAL cells (4B). These "outlier" samples were from the same subject. Of note, this individual displayed positive responses in both PPD testing and QFN testing for LTBI; in contrast, neither of the two LTBI subjects with negative QFN testing proved to be an outlier in terms of expression of this gene signature. It was also notable that the pattern of clustering of expression within the 47 genes of the CD4-signature (y-axis of both figures) was substantially different between the *Mtb*-naïve and LTBI subjects, so that presentation of these findings in separate figures most accurately represents the results for each subject group.

Application of this model also allows for the derivation of classical measures of prediction performances for each subject group. For the *Mtb*-naïve subjects, the cluster-based prediction of infected vs. uninfected BAL samples demonstrated Area Under the Receiver Operating Characteristic Curve (AUC) of 91.7%, Specificity 83.3%, and Sensitivity 100%. For LTBI subjects, cluster-based prediction of memory (unsorted *Mtb*-infected) vs. "memoryless" (unsorted, uninfected and CD4-depleted, *Mtb* infected) samples display AUC 95.5%, Specificity 90.9%, and Sensitivity 100%.

Networks

Analysis of gene expression networks was performed as well; as with pathway analysis, the role of resident airway CD4+ T cells was substantial. As illustrated in Figure 5, the top 3 networks identified in analysis of gene expression response of unsorted BAL cells from individuals with LTBI were i) "infectious diseases; endocrine system disorders; gastrointestinal disease", ii) "antimicrobial response; inflammatory response; cancer", and iii) "cellular function and maintenance, hematological system development and function; cellular development". Gene expression within each of these networks was substantially reduced in BAL cells from which CD4+ T cells were depleted prior to *Mtb* infection and in unsorted BAL from *Mtb*-naïve subjects, as illustrated. In contrast, the top 3 gene expression networks observed in CD4+ T-cell depleted BAL cells were i) "lipid metabolism, small molecule biochemistry, vitamin and mineral metabolism", ii) "cellular movement, hematological system development and function, immune cell trafficking", and iii) "infectious diseases, hematological disease, immunological disease" (not shown).

In addition, we used the 47-gene signature to develop our own gene expression network specific to the role of CD4+ T cells in defining the global *Mtb*-induced gene expression profile of LTBI. As illustrated in Figure 6, this novel network centers on IFNγ and displays connections to all but 2 of the 47 genes identified through pathway analysis. As anticipated by the manner in which the component genes of the network were identified, only limited expression of these genes is observed within the network for either LTBI subjects following CD4 T-cell depletion, or for *Mtb*-naïve subjects. Assessment of intra-class correlation (ICC) of this *Mtb*-induced gene expression network within the 3 study conditions indicated that there was a highly significant correlation between study the conditions of CD4-depleted samples from LTBI subjects and unsorted BAL cells from *Mtb*-naïve individuals (p=2.27e-05). In contrast, ICCs of this network between unsorted BAL cells and CD4-depleted BAL cells from LTBI subjects and between unsorted LTBI BAL and unsorted *Mtb*-naïve BAL were not significant (p=0.315 and p=0.196, respectively).

Mtb-induced cytokine production and polyfunctionality of Mtb-responsive CD4+ T-cells in LTBI

Because the dominance of IFNγ-induced responses in the CD4 T-cell mediated gene signature in LTBI contrasted with prior reports suggesting the importance of localization of polyfunctional CD4+ T cells to the lungs in immunity to *Mtb*, we assessed production of multiple CD4+ T-cell associated cytokines by BAL cells of LTBI individuals (Figure 7). First, we evaluated the supernatants of cell cultures used in the gene expression analysis for production of various T-cell associated cytokines. As illustrated, IFNγ, TNFα, IL-2 and

IL-17 were all produced by BAL cells from LTBI subjects. Depletion of CD4+ T cells from cultures resulted in significant decreases in *Mtb*-induced production of IFNγ, IL-2 and IL-17. TNFα production was decreased following CD4+ T-cell depletion as well, although not significantly so (7A). In contrast, CD8 depletion did not result in significant changes in production of any of these cytokines (not shown).

Because evaluation of BAL cell culture supernatants from LTBI subjects demonstrated production of multiple T-cell associated cytokines, we then evaluated the polyfunctionality of BAL CD4+ T cells in these individuals. In prior studies, we demonstrated that CD4+ BAL T cells overwhelmingly express an effector-memory (T_{EM}) phenotype [14]; we found this to be true with the current LTBI subjects as well, as >95% of all BAL CD4+ T cells were CD45RA- and CCR7-. Accordingly, our analysis is focused on this population. Figure 7B indicates the percentage of CD4+ T_{EM} cells from each subject displaying PPD-induced production of each of the 15 potential combinations of these 4 cytokines IFNγ, TNFα, IL-2, and IL-17, and the color scheme below each combination indicates the shading of the corresponding pie graph "slice" as shown in the graphic summary of Figure 7C. The very low percentage of cells that produced all 4 cytokines is represented by the very thin black slice pointing straight up in the figure; from there, the proportions of the various combinations of 3 cytokines, 2 cytokines, and a single cytokine proceed clockwise in the same order presented in the 7B. The colored arcs surrounding the pie graph represent each of the cytokines evaluated, as detailed in the figure legend. As indicated, nearly all PPD-responsive CD4+ T_{EM} produced TNFα, whereas more than half produced IFNγ. Of the IFNγ producing CD4+ T_{EM}, the great majority also showed positive staining for TNFα, whereas approximately 25% showed polyfunctional production IFNγ, TNFα and IL-2. In contrast, very few cells demonstrated PPD-induced production of IL-17, consistent with the low levels of IL-17 detected in culture supernatants.

DISCUSSION

The recent introduction of genome-wide gene expression to the assessment of vaccine responses had provided a comprehensive means of assessing the global impact of immunization [48–49]. Likewise, developments in mucosal immunology and mucosal vaccinology have indicated the importance of responses at the sites of initial pathogen exposure in mediating protection [50–53]. With regard to immune responses to respiratory pathogens, airborne infections have been demonstrated to induce populations of lung-resident memory T cells that do not rejoin the general circulation [54]. In murine models of *Mtb* infection in particular, CD4+ tissue resident-memory cells (T_{RM}) provide more effective protection against respiratory reinfection than do circulating CD4+ T cells associated with the pulmonary vasculature [11]. Multiple investigators have demonstrated that aerosol vaccination may be optimal for inducing protective immunity to *Mtb* in association with the increased early localization of *Mtb*-responsive CD4+ T cells to the airways [9–10, 16–17]. In particular, development of polyfunctional CD4+ T cells capable of *Mtb*-induced production of IFNγ, TNFα and IL-2 within the airways has been suggested to provide optimal protection from respiratory challenge with *Mtb* [19–20]. These studies further emphasize the importance of assessing *Mtb*-specific immune responses in the airways of human subjects.

In human studies, sampling of airway immune cells via bronchoalveolar lavage provides a safe, well-tolerated means to assess local immunity within the lung. Cells of the airway also provide the first line of defense against infection from respiratory pathogens such as *Mtb*. Study of BAL cells from healthy individuals with LTBI demonstrates how *Mtb*-specific immunity that has established following respiratory exposure to the organism provides initial recall responses at the time of re-exposure to the organism. We have previously demonstrated that, compared to peripheral blood, BAL cells in LTBI are markedly enriched for CD4+ T cells that are responsive to protein antigens of *Mtb*. Specifically, we found that an average of 5% of BAL CD4+ T cells in baseline BAL of LTBI subjects were capable of IFNγ production in response to in vitro stimulation with PPD. Further, production of IFNγ by these cells results in rapid local production of IFNγ-inducible chemokines that can recruit additional immune cells to the airways in response to re-exposure to the organism [14]. In the current study, we sought to evaluate the more global impact of resident T cells in the lungs on initial responses to respiratory re-exposure to *Mtb*.

Our findings demonstrate that *Mtb*-responsive CD4+ T cells localized to the airways play a predominant role in the initial response of BAL cells from LTBI subjects. Specifically, a signature composed of 47 *Mtb*-induced genes was identified as defining the impact of local CD4+ T-cells in initial recall responses to *Mtb*. These genes were components of 12 canonical pathways that are identified to a level of significance at least 2 logs greater in unsorted BAL cells from LTBI subjects than in paired CD4+ T-cell depleted BAL cells from these same subjects. The 12 pathways were also identified with 2 logs greater significance in LTBI subjects than in *Mtb*-naïve controls. Of 68 genes within these pathways, each of the 47 signature genes were also expressed with 2 log lower p-values in CD4-depleted samples from LTBI subjects and unsorted BAL cells of *Mtb*-naïve subjects than in unsorted LTBI BAL cells. In contrast, depletion of CD8+ T cells from BAL cells of LTBI subjects did not identify any genes that met all components of this stringent set of criteria.

Prior studies of global gene expression in *Mtb* have largely focused on differentiating individuals with LTBI from those with active tuberculosis, or on defining the gene expression profiles of specific populations of *Mtb*-specific T-cells [55–58]. In contrast, our study is the first to examine the global response to *Mtb* re-exposure within the mixture of airway-resident immune cells that are the first to encounter the organism. Given that lymphocytes typically represent only 5–10% of cells in baseline BAL of healthy individuals, *Mtb*-responsive CD4+ T cells account for <1% of all baseline BAL cells even in individuals in whom these antigen-specific cells represent as many as 10% of all airway CD4+ T cells. Assessment of global gene expression of BAL cells thus overwhelming reflects alterations in the mRNA of alveolar macrophages (AM). Our findings that local IFNγ production by resident CD4+ T cells of the airways so profoundly alters overall BAL cell gene expression indicates the remarkable impact of 1% or fewer airway cells in determining the initial immune response to re-exposure to *Mtb*. Although IFNγ is central to the novel immune network constructed from this gene signature, our findings do not exclude the possibility that the polyfunctional nature of resident BAL CD4+ T cells in LTBI may be critical to optimal protection from airborne *Mtb* in humans, as has been suggested in mice [19–20]. In prior studies, the induction of T-cell populations that display both effector function and proliferative capacity has been noted to be critical to protective immunity [59–60]; further,

in previous human studies we found that antigen-specific T-cell proliferation provides the greatest overall correlation with other assays of TB immunity [61]. It may therefore be that IL-2-production in the airways contributes to this signature by maintaining the local population of effector CD4+ T cells despite its lack of clear impact on the overall BAL cell gene expression profile. Likewise, *Mtb*-induced production of TNFα by polyfunctional airway CD4+ T cells may optimize protection by enhancing phagocyte responsiveness to IFNγ rather than through its direct impact of BAL cell gene expression [62]. A more puzzling finding is the increased significance of IL-17 associated pathways following CD4 depletion, even though the low levels of *Mtb*-induced IL-17 produced by unsorted BAL cells from LTBI was significantly reduced by this depletion. Neutrophils are among other cell populations in BAL and lung tissue potentially capable of IL-17 production [63]. We also speculate that the dominant effects of IFNγ could potentially inhibit the impact of IL-17 within this local environment; in this scenario the substantial decline in IFNγ-induced responses following CD4 depletion could permit more significant responses to IL-17 despite decreased production of this cytokine.

It should be noted that the twelve canonical pathways identified as being significantly impacted by CD4+ T-cell depletion in LTBI subjects emphasize the complexities of the IFNγ-centered network developed from this gene expression profile. Specifically, the impact of IFNγ in the airway environment is clearly pleiotropic in ways that reflect the contributions of multiple components of the immune system to protection from *Mtb*. Besides pathways specifically associated with Th1 immunity, multiple top pathways are notable for involving interactions of innate and acquired immunity, and for indicating the impact of IFNγ on antigen processing and presentation, stimulation of other lymphocyte populations (including CD8+ and NK cells), and promotion of mechanisms of cytoxicity. These include “Crosstalk between dendritic cells and natural killer cells”, “Antigen presentation pathway”, “Primary immunodeficiency signaling”, “Allograph rejection signaling”, “Graft vs. host disease signaling” and “Role of MAPK signaling in the pathogenesis of influenza”. The identification of “Type I diabetes mellitus signaling” as a pathway associated with this dataset is based on the contributions to these multiple immune mechanisms as well, although within the airways of LTBI subjects these responses clearly do not target pancreatic islet cells as they do in diabetes. The “Pathogenesis of multiple sclerosis” pathway was identified by the expression of multiple chemokine genes; in particular, the trio of IFNγ-inducible chemokines CXCL9 (Mig), CXCL10 (IP-10), and CXCL11 (I-TAC) identified in this pathway are relevant to known host defense mechanisms in TB because of their capacity to recruit of protective T-cell populations expressing their target receptor, CXCR3 [11, 64]. The “Retinoic acid mediated apoptosis signaling” pathway is also relevant to host immunity to *Mtb* in that extensive literature suggests multiple mechanisms by which Vitamin A can contribute to inhibition of the organism; these may include reduction of intracellular cholesterol (which serves as an energy source for *Mtb*), promotion of lysosomal acidification, and increasing reactive oxygen species and autophagy [65–67]. Indeed, a recent study has demonstrated the potential efficacy of inhaled all trans-Retinoic acid (ATRA), the active metabolite of vitamin A, as a TB treatment [68]. Identification of remaining pathway, “Protein ubiquitination” was based on the expression of multiple IFNγ-associated genes that contribute to the immunoproteasome [69]. This component of the

immune system degrades ubiquitinated proteins (of pathogens, in particular) for presentation via MHC Class I molecules to CD8+ T-cells and has been associated with protective immune responses to multiple viruses [70–71], although not specifically with *Mtb* infection.

A major obstacle to our approach is the limited numbers of BAL cells available for these studies, particularly in light of the large amount of cell loss associated with T-cell depletion protocols. This limitation made us unable to assess *Mtb*-induced BAL cell gene expression at multiple time points within studies of a specific individual. Assessment of predicted upstream regulators provides one means to ameliorate this shortcoming. As with the main body of analysis, upstream regular assessment again demonstrated the much greater impact of depletion of CD4+ T cells than CD8+ T cells to local *Mtb*-induced gene expression, and also emphasized an early role for Type I IFNs in this response. These findings are in contrast with multiple prior studies of peripheral blood gene expression of both humans with LTBI and animal models of *Mtb.* These investigations have suggested a dichotomy between immune signatures dominated by IFNγ and associated with continued control of the organism, versus those dominated by Type I IFNs and predictive of progression to active disease [57, 72–73]. Although complicated by the overlapping downstream responses to IFNγ and IFNα/β, our findings suggest that both types of IFNs can contribute in rapid sequence to presumably protective local recall responses to *Mtb*. The contrast also reflects the differing goals of these prior studies and our current project. Longitudinal studies of *Mtb*-infected individuals seek to identify markers of risk for progression to active disease. However, even peripheral immune markers that may be very useful in this setting do not necessarily reflect local immune events within the lung. As one example, pulmonary sarcoidosis, which shares both pathologic and immunologic features with tuberculosis [74] has long been noted for demonstrating compartmentalization of the immune response, in which active Th1-associated inflammation within the lung is actually associated with peripheral anergy and inverted blood CD4:CD8 ratios [75].

Our approach aims to define the initial local immune responses of *Mtb*-immune individuals to respiratory re-exposure to the organism, with the goal of application of this approach to initial evaluations of the potential efficacy of novel approaches to TB vaccination. Recent array-based findings by Hoft and colleagues have indicated that the immune signatures of CD4+ T cells of peripheral blood following BCG vaccination by standard intradermal and investigational PO administration are distinct; further, the degree to which these mycobacteria-specific T cells are localized to the airways is greater following oral as opposed to ID administration [76]. The findings thus suggest that the impact of localized *Mtb*-responsive CD4+ T cells within BAL cells that first encounter *Mtb* may be both qualitatively and quantitatively altered by the route of vaccination. The signature of 47 genes identified in our study provides a succinct profile of local immunity to *Mtb* in LTBI subjects, in whom initial exposure to the organism via inhalation may be expected to result in optimal localization of responsive CD4+ T cells to the lung. These findings can serve as a standard for comparison with human pulmonary immune responses induced by current intradermal vaccination with BCG and by novel TB vaccines and vaccine strategies. Correlation of these observations with those from animal models in which the results of *in vivo* infection can be directly assessed will likely be required to confirm which vaccine approaches and resulting

local gene expression profiles most optimally predict protection from respiratory infection with *Mtb*.

Supplementary Material

Refer to Web version on PubMed Central for supplementary material.

Acknowledgments

Sources of Funding:

NIH RO1 HL-111523 and VA Merit Review CX001283 (to RFS)

NIH RO1 AI-080313 (to DHC)

All research bronchoscopies were performed in the William T. Dahms Clinical Research Unit, which is a facility of the CWRU Clinical and Translational Science Collaborative (CTSC) which is funded by NIH UL1 TR-000439. Luminex assays were performed in the Bioanalyte Core, which is also a component of the CTSC. Infections with virulent *Mtb* were performed in the Elizabeth Rich Biosafety Level 3 Facility, which is a Core facility of the CWRU Center for AIDS Research (CFAR) which is supported by P30 AI036219. Microarray studies were supported by the Gene Expression and Genotyping Facility, a component of the Integrated Genomic Shared Resource sponsored by the Case Comprehensive Cancer Center (P30 CA43703). Analysis of microarray data made use of the High-Performance Computing Cluster in the Core Facility for Advanced Research Computing at CWRU.

REFERENCES

1). World Health Organization. 2018 Global Tuberculosis Report 2018. Geneva, Switzerland: World Health Organization.

2). Schluger NW and Rom WN. 1998 The host immune response to tuberculosis. Am. J. Resp. Crit. Care Med 157: 679–691. [PubMed: 9517576]

3). Fine PE. 1989 The BCG story: lessons from the past and implications for the future. Rev. Infect. Dis 11: S353–359. [PubMed: 2652252]

4). Brewer TF. 2000 Preventing tuberculosis with bacillus Calmette-Guérin vaccine: a meta-analysis of the literature. Clin. Infect. Dis 31: S64–77. [PubMed: 11010824]

5). Hoft DF. 2008 Tuberculosis vaccine development: goals, immunologic design, and evaluation. Lancet. 372: 164–175. [PubMed: 18620952]

6). Zhu B, Dockrell HM, Ottenhoff THM, Evans TG, and Zhang Y. 2018 Tuberculosis vaccines: opportunities and challenges. Respirol. 23: 359–368.

7). Bhatt K, Verma S, Ellner JJ, Salgame P. 2015 Quest for correlates of protection against tuberculosis. Clin. Vaccine Immunol 22: 258–266. [PubMed: 25589549]

8). Satti I and McShane H. 2019 Current approaches towards identifying a correlate of human protection from tuberculosis. 18: 43–59

9). Chackerian A, Perera T, and Behar S. 2001 Gamma interferon-producing CD4+ T lymphocytes in the lung correlate with resistance to infection with Mycobacterium tuberculosis. Infect. Immun; 69: 2666–2674. [PubMed: 11254633]

10). Santosuosso M, McCormick S, Zhang X, Zganiacz A and Xing Z. 2006 Intranasal boosting with an adenovirus-vectored vaccine markedly enhances protection by parenteral Mycobacterium bovis BCG immunization against pulmonary tuberculosis. Infect. Immun, 74: 4643–4643

11). Sakai S, Kauffman KD, Schenkel JM, McBerry CC, Mayer-Barber KD, Masopust D, Barber DL. 2014 Cutting edge: control of Mycobacterium tuberculosis infection by a subset of lung parenchyma-homing CD4 T cells. J Immunol.; 192: 2965–2969. [PubMed: 24591367]

12). Andersen P, Urdahl KB. 2015 TB vaccines; promoting rapid and durable protection in the lung. Curr Opin Immunol. 35: 55–62. [PubMed: 26113434]

13). Silver RF, Li Q, Zukowski L, Kotake S, Pozuelo F, Krywiak A, and Larkin R. 2003 Recruitment of antigen-specific Th1-like responses to the human lung following segmental antigen challenge

with Purified Protein Derivative of M. tuberculosis. Am. J. Resp. Cell. and Mol. Biol, 29: 117–123.

14). Walrath J, Zukowski L, Krywiak A, and Silver RF. 2005 Resident Th1-like effector-memory cells in pulmonary recall responses to Mycobacterium tuberculosis. Am. J. Resp. Cell. and Mol. Biol, 33: 48–55.

15). Walrath JR and Silver RF. 2011 The α4β1 integrin in localization of Mycobacterium tuberculosis-specific Th1 cells to the human lung. Am. J. Resp. Cell. Mol. Biol 45: 24–30.

16). Wang J, Thorson L, Stokes RW, Santosuosso M, Huygen K, Zganiacz A, Hitt M, Xing Z. 2004 Single mucosal, but not parenteral, immunization with recombinant adenoviral-based vaccine provides potent protection from pulmonary tuberculosis. J. Immunol, 173: 6357–6365. [PubMed: 15528375]

17). Santosuosso M, Zhang Z, McCromick S, Wang J, Hitt M and Xing Z. 2005 Mechanisms of mucosal and parenteral tuberculosis vaccination: adenoviral-based mucosal immunization preferentially elicits sustained accumulation of immune protective CD4 and CD8 positive T cells within the airway lumen. J. Immunol, 174: 7986–7994. [PubMed: 15944305]

18). Goter-Robinson C, Derrick SC, Yang AL, Jeon BY, Morris SL. 2006 Protection against an aerogenic Mycobacterium tuberculosis infection in BCG-immunized and DNA-vaccinated mice is associated with early type I cytokine responses. Vaccine. 24: 3522–3529. [PubMed: 16519971]

19). Forbes EK, Sander C, Ronan EO, McShane H, Hill AV, Beverly PC, Tchilian EZ. 2008 Multifunctional, high-level cytokine-producing Th1 cells in the lung, but not spleen, correlate with protection against Mycobacterium tuberculosis aerosol challenge in mice. J. Immunol 181: 4955–4964. [PubMed: 18802099]

20). Lindenstrom T, Agger EM, Korsholm KS, Darrah PA, Aagaard C, Seder RA, Rosenkrands I, Andersen P. 2009 Tuberculosis subunit vaccination provides long-term protective immunity characterized by multifunctional CD4 memory T cells. J. Immunol 182: 8047–8055 [PubMed: 19494330]

21). Lewinsohn DA, Lewinsohn DM and Scriba TJ 2017 Polyfunctional CD4+ T cells as targets for tuberculosis vaccination. Frontiers in Immunol. 8: 1262.

22). Khader S, Bell G, Pearl J, Fountain J, Rangel-Moreno J, Cilley G, Shen F, Eaton SM, Gaffen SL, Swain SL, Locksely RM, Haynes L Randall TD and Cooper AM. 2007 IL-23 and IL-17 in the establishment of protective pulmonary CD4+ T cell responses after vaccination and during Mycobacterium tuberculosis challenge. Nat. Immunol 8: 369–377. [PubMed: 17351619]

23). Wu Y, Woodworth JS, Shin DS, Morris S, Behar SM. 2008 Vaccine-elicited 10-kildalton culture filtrate protein-specific CD8+ T cells are sufficient to mediate protection against *Mycobacterium tuberculosis* infection. Infect. Immun 76: 2249–2255. [PubMed: 18332205]

24). Torrado E and Cooper AM. 2010 IL-17 and Th17 cells in tuberculosis. Cytokine & Growth Factor Rev. 21: 455–462. [PubMed: 21075039]

25). Lyadova IV and Panteleev AV. 2015 Th1 and Th17 cells in tuberculosis: protection, pathology, and biomarkers. Med. Inflamm 854507.

26). Coulter F, Parrish A, Manning D, Kampmann B, Mendy J, Garand M, Lewinsohn DM, Riley EM and Sutherland JS. 2017 IL-17 production from T helper 17, mucosal-associated invariant T and γδ cells in tuberculosis infection and disease. Front. Immunol, 8: 1252 [PubMed: 29075255]

27). Lempp JM, Zajdowicz J, Hankinson AL, Toney SR, Keep LW, Mancuso JD, and Mazurek GH Assessment of the QuantiFERON Gold In-Tube test for the detection of Mycobacterium tuberculosis infection in United States Nave recruits. 2017, PLoS One, 12(5): e0177752 10.1371/journal/pone.0177752. [PubMed: 28545136]

28). Silver RF, Li Q, Boom WH, Ellner JJ. 1998 Lymphocyte-dependent inhibition of growth of virulent Mycobacterium tuberculosis within human monocytes: requirement for CD4+ T cells in purified protein derivative-positive, but not in purified protein derivative-negative subjects. J. Immunol, 160: 2408–2417 [PubMed: 9498784]

29). Canaday DH, Sridaran S, Van Epps P, Aung H, Burant CJ, Nserko M, Mayanja-Kizza H, Betts MR, and Toossi Z. 2015 CD4+ T cell polyfunctional profile in HIV-TB coinfection are similar between individuals with latent and active TB infection. Tuberculosis, 95: 470–475. [PubMed: 25956974]

30). Benjamini Y, and Hochberg Y 1995 Controlling the false discovery rate: a practical and powerful approach to multiple testing. J R Statist Soc 57: 289–300.

31). Liu P, and Hwang JT 2007 Quick calculation for sample size while controlling false discovery rate with application to microarray analysis. Bioinformatics (Oxford, England) 23: 739–746.

32). Storey JD 2002 A direct approach to false discovery rates. J R Statist Soc 64(3): 479–498.

33). Storey JD 2003 The positive false discovery rate: A Bayesian interpretation and the q-value. The Annals of Statistics 31: 2013–2035.

34). Dazard J-E, and Rao JS 2012 Joint Adaptive Mean-Variance Regularization and Variance Stabilization of High Dimensional Data. Comput Stat Data Anal 56: 2317–2333. [PubMed: 22711950]

35). Dazard J-E, and Rao JS 2010 Regularized Variance Estimation and Variance Stabilization of High Dimensional Data. Proceedings. American Statistical Association Meeting 2010: 5295–5309.

36). Dazard J-E, Xu H, and Rao JS 2011 R package MVR for Joint Adaptive Mean-Variance Regularization and Variance Stabilization. Proceedings. American Statistical Association. Meeting 2011: 3849–3863.

37). Papana A, and Ishwaran H 2006 CART variance stabilization and regularization for high-throughput genomic data. Bioinformatics (Oxford, England) 22: 2254–2261.

38). Ishwaran H, and Rao JS 2003 Detecting differentially expressed genes in microarrays using Bayesian model selection. J Amer Stat Assoc 98: 438–455.

39). Ishwaran H, and Rao JS 2005 Spike and slab gene selection for multigroup microarray data. J Amer Stat Assoc 100: 764–780.

40). Ishwaran H, and Rao JS 2005 Spike and slab variable selection: frequentist and Bayesian strategies. The Annals of Statistics 33: 730–773.

41). Genovese C, and Wasserman L 2002 Operating characteristics and extensions of the false discovery rate procedure. J R Statist Soc 64: 499–517.

42). Ishwaran H, Rao JS, and Kogalur UB 2006 BAMarraytrade mark: Java software for Bayesian analysis of variance for microarray data. BMC bioinformatics 7: 59. [PubMed: 16466568]

43). Bartko JJ 1966 The intraclass correlation coefficient as a measure of reliability. Psychological Reports 19: 3–11. [PubMed: 5942109]

44). McGraw KO, and Wong SP 1996 Forming inferences about some intraclass correlation coefficients. Psychological Methods 1: 30–46.

45). Shrout PE, and Fleiss JL 1979 Intraclass correlation: uses in assessing rater reliability. Psychological Bulletin 86.

46). Schwander S, Torres M, Sada E, Carranza C, Ramos E, Tary-Lehman M, Wallis RS, Sierra J, and Rich EA Enhanced responses to *Mycobacterium tuberculosis* antigens by human alveolar lymphocytes during active pulmonary tuberculosis. 1998 J. Infect. Dis, 178: 1434–1445. [PubMed: 9780265]

47). Tibshirani R 2001 Estimating the number of clusters in a data set via the gap statistic. J R Statist Soc 63: 411–423.

48). Querec TD, Akondy RS, Lee EK, Cao W, Nakaya HI, Teuwen D, Pirani A, Gernert K, Deng J, Marzolf B, Kennedy K, Wu H, Bennouna S, Oluoch H, Miller J, Vencio RZ, Mulligan M, Aderem A, Ahmed R, Pulendran B 2009 Systems biology approach predicts immunogenicity of the yellow fever vaccine in humans. Nat Immunol. 10:116–25. [PubMed: 19029902]

49). Pulendran B, Li S, and Nakaya HI 2010 Systems vaccinology. Immunity, 33:516–29. [PubMed: 21029962]

50). Holmgren J and Czerkinsky C 2005 Mucosal immunity and vaccines. Nature Med. 11: S45–S53. [PubMed: 15812489]

51). Shin H and Iwasaki A 2012 A vaccine strategy that protects against genital herpes by establishing local memory T cells. Nature. 491: 463–467. [PubMed: 23075848]

52). Belyakov IM, Ahlers JD 2012 Mucosal immunity and HIV-1 infection: applications for mucosal AIDS vaccine development. Curr. Top. Microbiol. Immunol 354: 157–179 [PubMed: 21203884]

53). Kumar B, Connors TJ and Farber DL 2018 Human T cell development, localization, and function throughout life. Immunity, 48: 202–213. [PubMed: 29466753]

54). Teijaro JR, Turner D, Pham Q, Wherry EJ, Lefrancois L and Farber DL 2011 Cutting edge: Tissue-retentive lung memory CD4+ T cells mediate optimal protection to respiratory virus infection. J. Immunol 187: 5510–5514. [PubMed: 22058417]

55). Jacobsen M, Repsilber D, Gutschmidt A, Neher A, Feldmann K, Mollenkoph HJ, Ziegler A, and Kaufmann SHE 2007 Candidate biomarkers for discrimination between infection and disease caused by Mycobacterium tuberculosis. J Mol. Med 85: 613–621. [PubMed: 17318616]

56). Sweeney TE, Breaviak L, Tato CM, and Khatri P 2016 Genome-wide expression for diagnosis of pulmonary tuberculosis: a multicohort analysis. Lancet Resp. Med 4: 213–224.

57). Zak DE, Penn-Nicholson A, Scriba TJ, Thompson E, Suliman S, Amon LM, Mahomed H, Erasmus M, Whatney W, Hussey GD, Abrahams D, Kafaar F, Hawkridge T, Verver S, Hughes EJ, Ota M, Sutherland J, Howe R, Dockrell HM, Boom WH, Thiel B, Ottenhoff THM, Mayanja-Kizza H, Crampin AC, Downing K, Hatherill M, Valvo J, Shankar S, Parida SK, Kaufmann SH, Walzl G, Aderem A, Hanekom WA 2016 A blood signature for tuberculosis disease risk: a prospective cohort study. Lancet 387: 2312–2322. [PubMed: 27017310]

58). Burel JG, Lindestram Arlehamn CS, Khan N, Seumois G, Greenbaum JA, Taplitz R, Gilman RH, Saito M, Pandurangan V, Sette A, and Peters B 2018 Transcriptomic analysis of CD4+ T cells reveals novel immune signatures of latent tuberculosis. J. Immunol 200: 3283–3290. [PubMed: 29602771]

59). Lauvau G, Vijh S, Kong P, Horng T, Kerksiek K, Serbina N, Tuma RA, and Pamer EG 2001 Priming of memory but not effector CD8 T cells by a killed bacterial vaccine. Science. 294: 1735–1739 [PubMed: 11721060]

60). Migueles SA, Laborico AC, Shupert WL, Sabbaghian MS, Rabin R, Hallaha CW, Van Baarle D, Kostense S, Miedema F, McLaughlin M, Ehler L, Metcalf J, Liu S, and Connors M 2002 HIV-specific CD8+ T cell proliferation is coupled to perforin expression and is maintained in nonprogressors. Nat. Immunol 3: 1061–1066. [PubMed: 12368910]

61). Hoft DF, Worku S, Kampmann B, Whalen CC, Ellner JJ, Hirsch CS, Brown RB, Larkin R, Li Q, Yun H, and Silver RF 2002 I*nvestigation of the relationships between immune-mediated inhibition of mycobacterial growth and other potential surrogate markers of protective Mycobacterium tuberculosis immunity*. J. Inf. Dis 186: 1448–1457. [PubMed: 12404160]

62). Mosser DM and Edwards JP 2008 Exploring the full spectrum of macrophage activation. Nat. Rev. Immunol 12: 958–969.

63). Taylor PR, Bonfield TL, Chmiel JF,Pearlman E Neutrophils from F508del cystic fibrosis patients produce IL-17A and express IL-23-dependent IL-17RC. 2016 Clin. Immunol 170: 53–60. [PubMed: 27155366]

64). Arlehamn CL, Seumois G, Gerasimova A, Huang C, Fu Z, Yue X, Sette A, Vijayanand P, Peters B 2014 Transcriptional profile of tuberculosis antigen-specific T cells reveals novel multifunctional features. J Immunol. 193: 2931–2940. [PubMed: 25092889]

65). Wheelwright M, Kim EW, Inkeles MS, De Leon A, Pellegrini M, Krutzik SR, and Liu PT All-trans retinoic acid-triggered antimicrobial activity against *Mycobacterium tuberculosis* is dependent on NPC2. 2014 J. Immunol 192: 2280–2290. [PubMed: 24501203]

66). Pandey AL and Sassetti CM Mycobacterial persistence requires the utilization of host cholesterol. 2008 PNAS (USA), 105: 4376–4380. [PubMed: 18334639]

67). Coleman MM, Basdeo SA, Coleman AM, Ni Cheallaigh C, Peral de Castro C, McLaughlin AM, Dunne PJ, Harris J and Keane J 2018 Am. J. Resp. Cell. Mol. Biol 59: 548–556.

68). O'Connor G, Krishnan N, Fagan-Murphy A, Cassidy J, O'Leary S, Robertson BD, Keane J O'Sullivan MP and Cryan S-A Inhalable poly(lactic-co-glycolic acid) (PLGA) microparticles encapsulating all-trans-Retinoic acid (ATRA) as a host-directed, adjunctive treatment for Mycobacterium tuberculosis infection. 2019 Eur. J. Pharm. and Biopharm 134: 153–165. [PubMed: 30385419]

69). Kimura H, Caturegli P, Takahashi M, and Suzuki K New insights into the function of the immunoproteasome in immune and nonimmune cells. 2015. J. Immunol. Res Article ID 541984, 10.1155/2015/541984.

70). Robek MD, Garcia ML, Boyd BS, and Chisari FV Role of immunoproteasome catalytic submits in the immune response to hepatitis B virus. 2007 J. Virology 81: 483–491. [PubMed: 17079320]

71). Hensley SE, Zanker D, Dolan BP, Hickman DA, Embry AC, Skon CN, Grebe KM, Griffin TA, Chen W, Bennink JR and Yewdell JW Unexpected role for the immunoproteasome subunit LMP2 in antiviral humoral and innate immune responses. 2010 J. Immunol, 184: 4115–4122. [PubMed: 20228196]

72). Ottenhoff THM, Dass RH, Yang N, Zhang MM, Wong HEE, Sahiratmadja E, Khor CC, Alisjahbana B, van Crevel R, Marzuki S, Seielstad M, van de Vosse E and Hibberd ML Genome-wide expression profiling identifies Type 1 interferon response pathways in active tuberculosis. 2012 PLoS One 7: e45839. doi:10.1371/journal.pone.0045839. [PubMed: 23029268]

73). Thompson EG, Shankar S, Gideon HP, Braun J, Valvo J, Skinner JA, Aderem A, Flynn JL, Lin PL and Zak DE Prospective discrimination of controllers from progressors early after low-dose Mycobacterium tuberculosis infection of cynomolgus macaques using blood RNA signatures. 2018 J. Inf. Dis 217:1318–1322. [PubMed: 29325117]

74). Grunewald J, Grutters JC, Arkema EV, Saketkoo LA, Moller DR and Muller-Quernheim J Sarcoidosis. 2019 Nat. Rev. Dis. Primers 5: 45 Doi: 10.1038/s41572-019-0096-x. [PubMed: 31273209]

75). Hunninghake GW, Crystal RG Pulmonary sarcoidosis—a disorder mediated by excess helper T-lymphocyte activity at sites of disease activity. 1981 NEJM. 305: 429–434. [PubMed: 6454846]

76). Hoft DF, Xia M, Zhang GL, Blazevic A, Tennant J, Kaplan C, Matuschak G, Dube TJ, Hill H, Schlesinger LS, Andersen PL and Brusic V 2018 PO and ID BCG vaccination in humans induce distinct mucosal and systemic immune responses and $CD4^+$ T cell transcriptomal molecular signatures. Mucosal Immunol. 11: 486–495. [PubMed: 28853442]

KEY POINTS

1. IFNγ dominates the CD4+ dependent *Mtb*-induced BAL cell gene signature in LTBI
2. Nevertheless, CD4+ BAL cells in LTBI display polyfunctional responses to *Mtb*
3. This signature may provide a means to assess vaccine-induced local immunity to *Mtb*

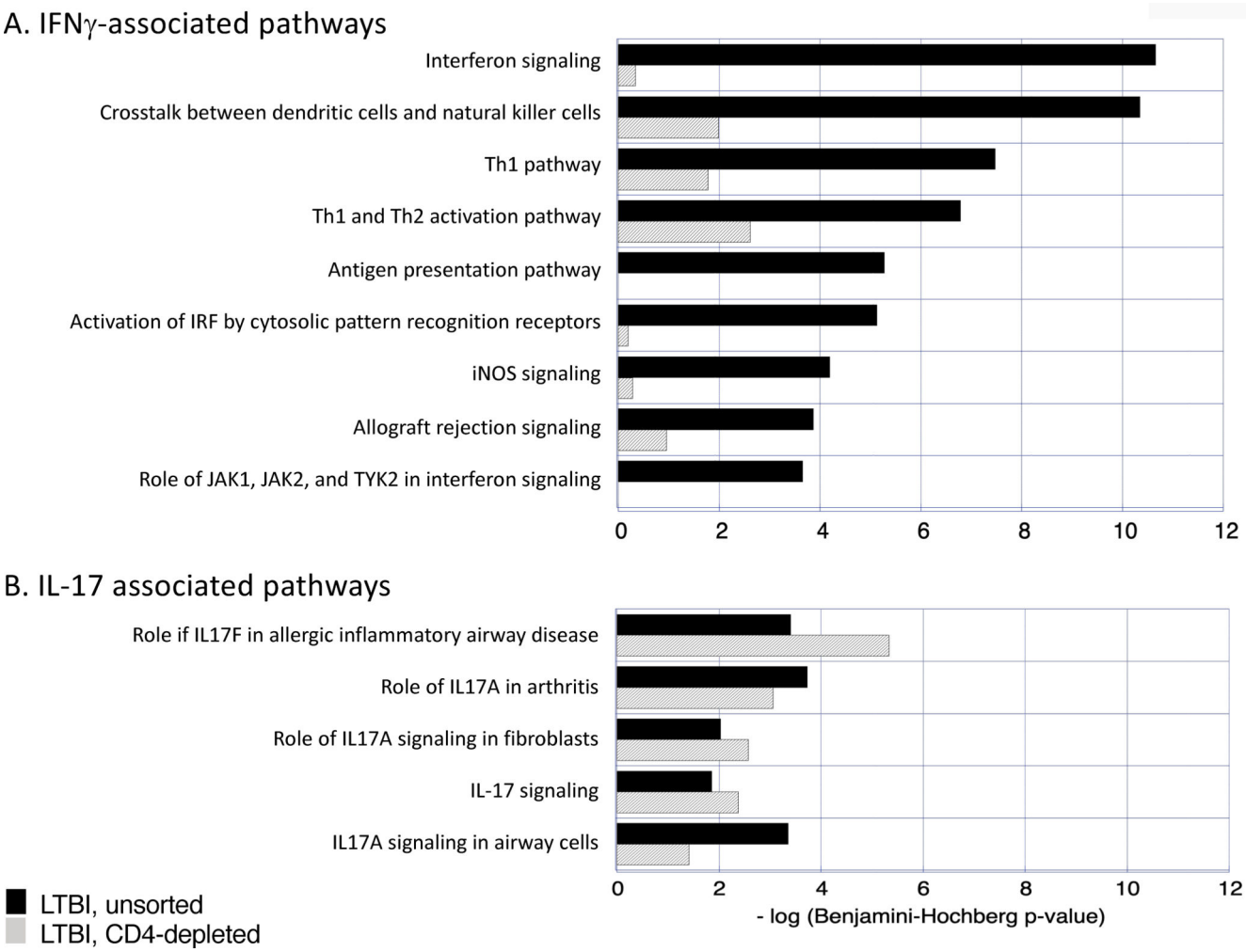

Figure 1:

CD4-depletion of BAL cells from LTBI subjects results in loss of significance of several *Mtb*-induced pathways associated with the impact of IFNγ production (1A); in contrast, the significance of pathways associated with IL-17 production are not reduced in CD4-depleted LTBI BAL samples (1B). In both figures, significance is expressed as -log (p-value). Dark blue bars represent findings from unsorted BAL cells whereas light blue bars represent p-values of *Mtb*-induced gene expression in BAL cells from which CD4+ T cells had been removed by magnetic bead sorting.

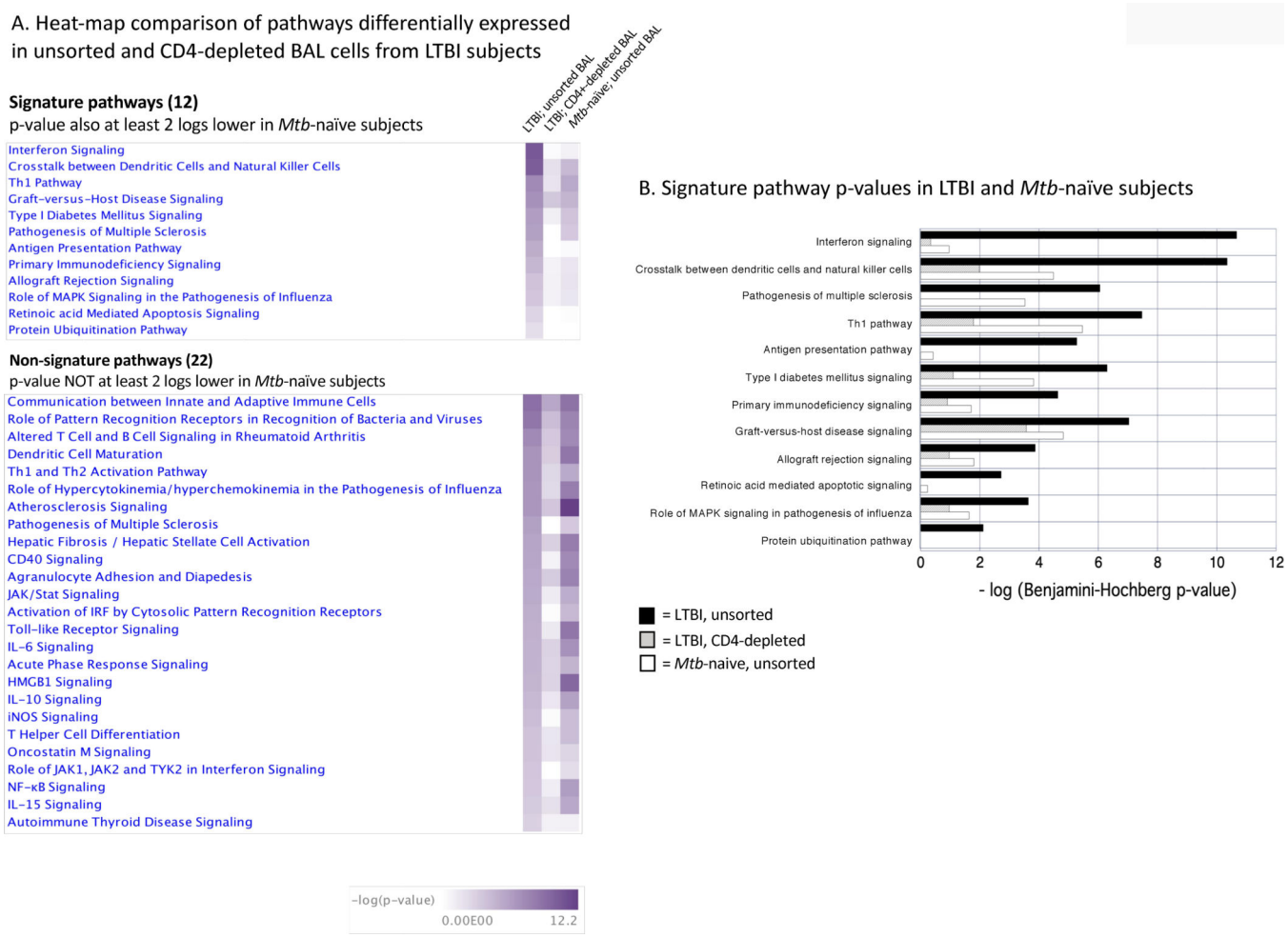

Figure 2:

BAL cell *Mtb*-induced canonical pathways that demonstrated a reduction in p-value of at least 2 logs following depletion of CD4+ T cells. Heat maps of -log (p-value) in unsorted BAL samples from LTBI subjects, CD4-depleted BAL cells from LTBI subjects, and unsorted BAL from *Mtb*-naïve subjects are presented in Figure 2A. For the 12 “signature” pathways (top), pathways significance was reduced by >2 logs in both LTBI BAL from which CD4+ T cells had been depleted and in *Mtb*-naïve subjects. For 22 “non-signature” pathways, decrease in -log (p-value) of >2 log was observed following CD4 depletion from LTBI BAL, but not in that of *Mtb*-naïve subjects. The -log p-values for 12 “signature” pathways are presented graphically in 2B. -log (p-values) for LTBI-unsorted BAL cells are presented in dark blue bars. Bars for LTBI CD4-depleted BAL cells are light blue and red bars represent -log (p-values) for unsorted BAL cells of *Mtb*-naïve subjects.

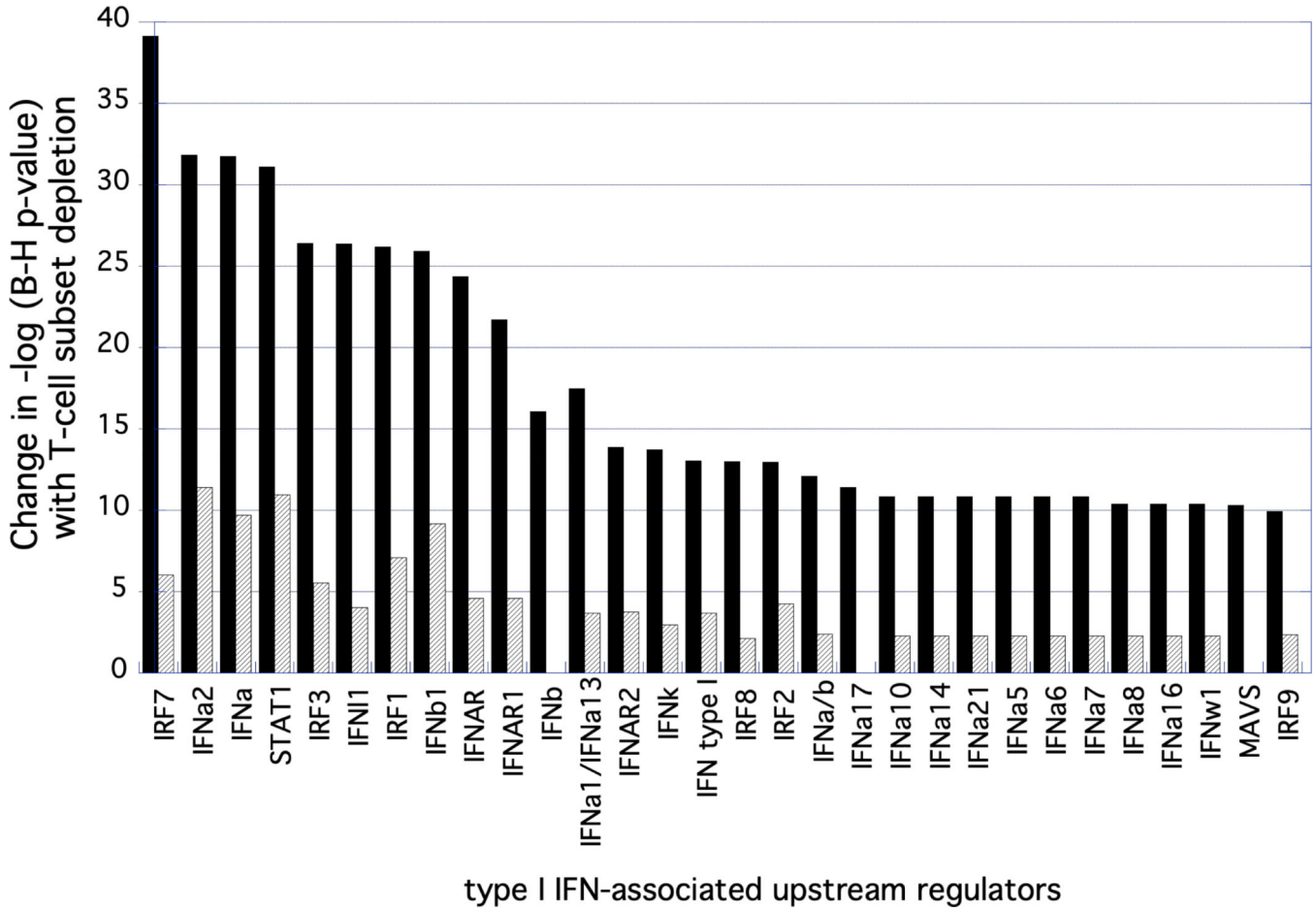

Figure 3:

Type I IFN-associated genes identified as impacted CD4+ and CD8+ T cells on *Mtb*-induced BAL cell gene expression in LTBI. The figure shows 30 Type I IFN-associated upstream regulators and the degree to which the significance of their associations with the dataset were altered by depletion of CD4+ (black) or CD8+ (gray) T cells, expressed as the change in -log of p-values. As indicated, although both T-cell subset depletion impacted the significance of multiple regulators, the magnitude of this effect was far greater for CD4+ T-cells that for CD8+ cells.

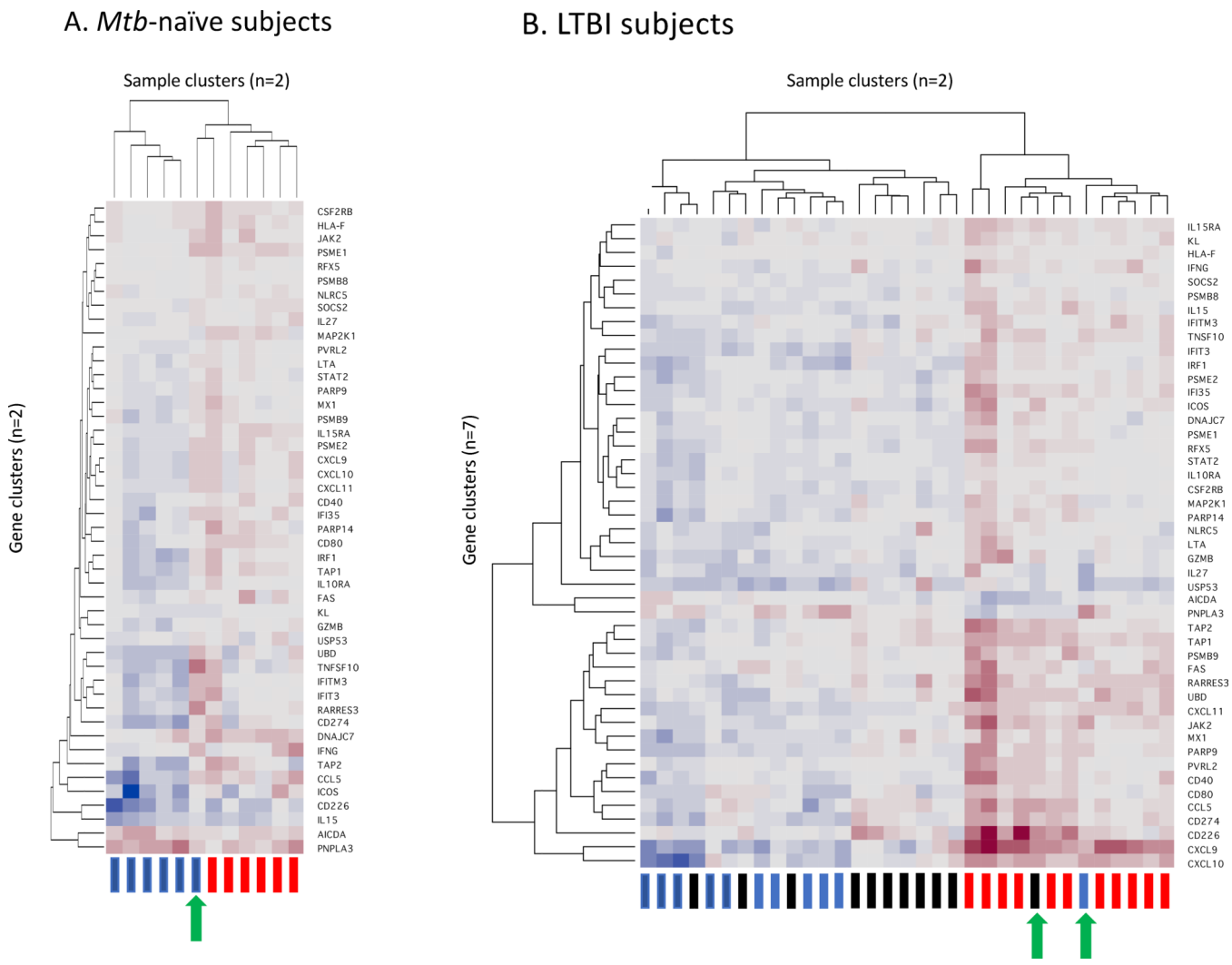

Figure 4:

Cluster analysis of expression of the 47 signature genes in *Mtb*-naïve subjects (4A) and individuals with LTBI (4B). Clustering was performed on a blinded basis according to patterns of responses of the 47-gene signature without regard to the study conditions of each sample. As illustrated in the y-axis of each figure, the clustering of the signature genes was substantially different in *Mtb*-naïve and LTBI subject groups, leading to the need to present the results in separate heat maps. As indicated on the x-axes, samples from each subject group were segregated into two clusters. In *Mtb*-naïve subjects (4A), uninfected samples are represented by blue rectangles, whereas *Mtb*-infected samples are indicated in red. This clustering effectively separates responses of uninfected vs *Mtb*-infected BAL cells, with the exception of one subject whose uninfected cells gave responses more typical of the *Mtb*-infected cells (green arrow). For each LTBI subject, three samples are represented, with blue again indicating unsorted, uninfected cells and red unsorted, *Mtb*-infected cells, whereas black rectangles indicate CD4-depleted, *Mtb*-infected BAL cells (4B). Despite the representation of three sample types, these responses remain classified into two clusters, reflecting that finding that *Mtb*-induced gene expression of the signature 47 genes following

CD4+ T cell depletion was largely the same as that observed in unsorted, uninfected BAL cells of the same individuals. Unsorted *Mtb*-infected BAL samples from all 11 LTBI subjects segregated to the same cluster, which also included a single uninfected sample, as well as a single sample infected following CD4 T-cell depletion (green arrows). Of note, both of these “outlier” samples were from the same individual.

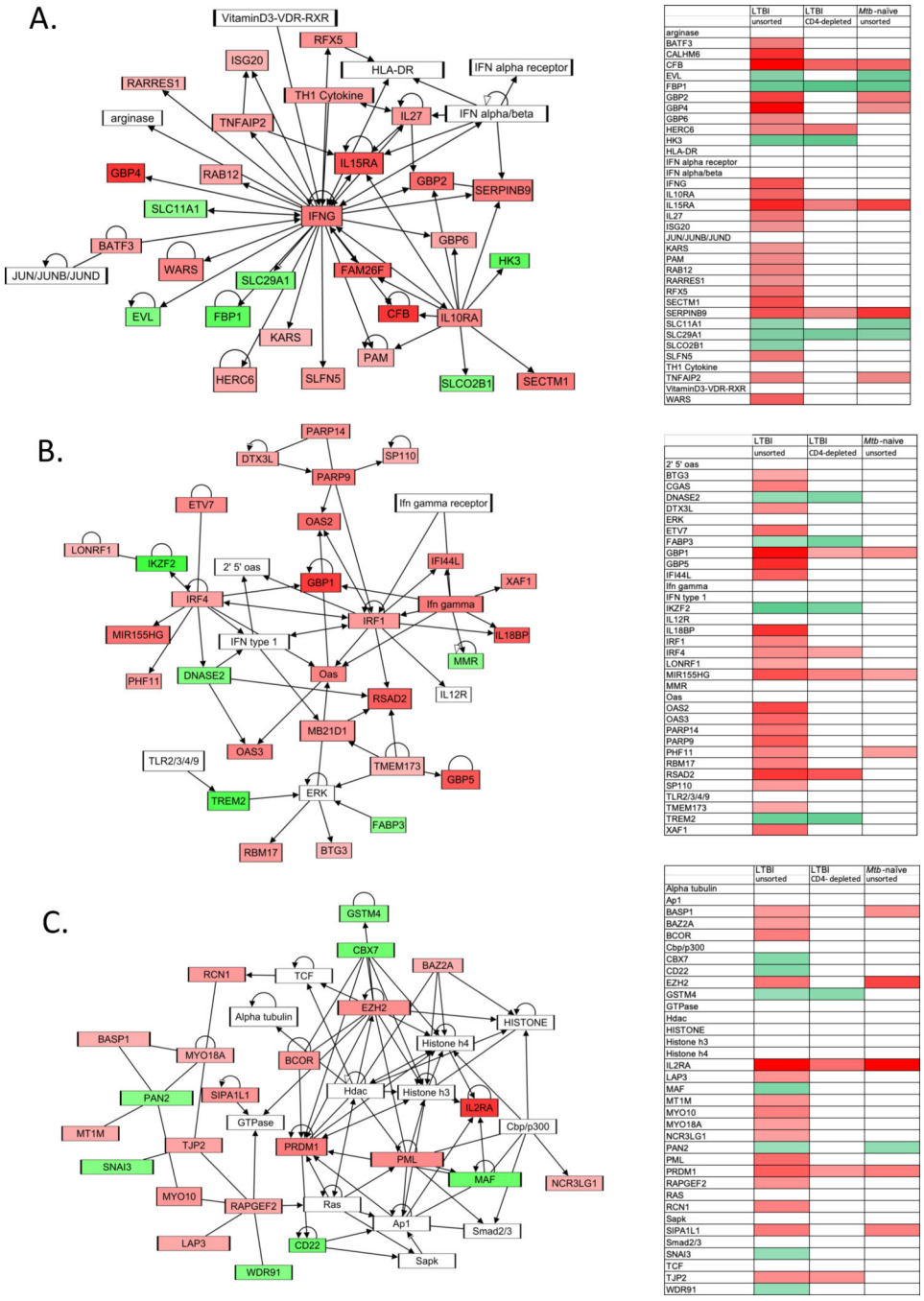

Figure 5.

The top networks identified through analysis of *Mtb*-induced BAL cell gene expression in LTBI subjects. Schematic figures illustrate gene interactions in these top 3 networks, A. “infectious diseases; endocrine system disorders; gastrointestinal diseases”, B. antimicrobial response; inflammatory response; cancer”, and C. “cellular function and maintenance, hematological system development and function; cellular development”. For each network figure (left), shading indicates degrees of significant upregulation (red) and downregulation (green) of gene expression in unsorted BAL cells from LTBI subjects. Heat maps to the right

of each figure indicate *Mtb*-induced expression of all network genes in this condition, as well as in CD4-depleted cells of LTBI subjects and unsorted BAL cells of Mtb-naïve controls.

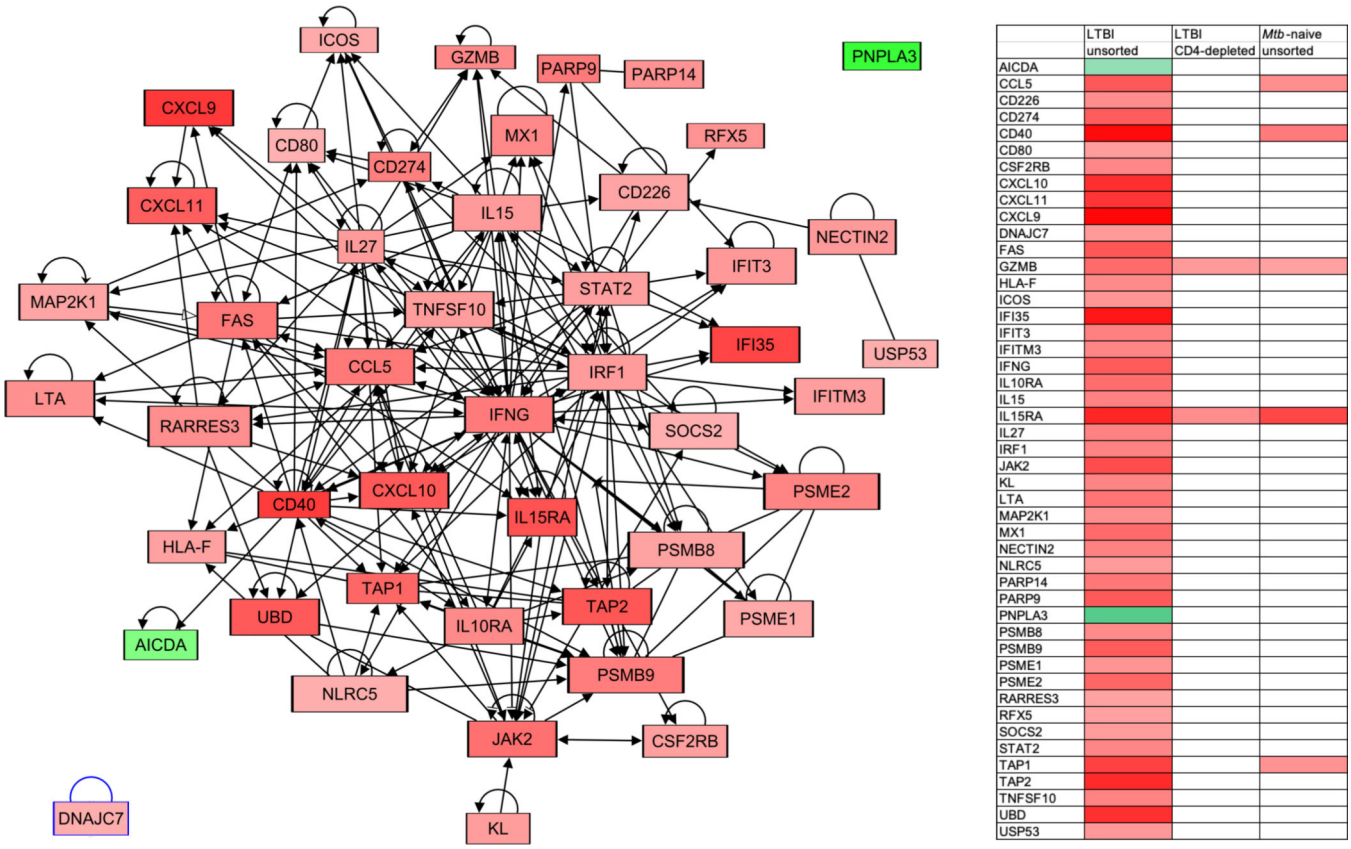

Figure 6:

Novel gene expression network representing the interrelationships of genes identified as the signature of CD4+ T-cell associated *Mtb*-induced gene expression in BAL cells from individuals with LTBI. Again, the figure represents gene expression in unsorted BAL samples from LTBI subjects; upregulated genes are represented with red shading and downregulated ones in green; as illustrated, all but 2 of the 47 genes within the identified signature have defined connections to a network that is centered on IFN**γ**. The associated heat map schematically compares expression of all network genes in this condition and in CD4+-depleted BAL cells from LTBI subjects and unsorted BAL cells from *Mtb*-naïve individuals using the same shading key. As indicted, significant *Mtb*-induced gene expression is almost completely absent within this network in these additional conditions.

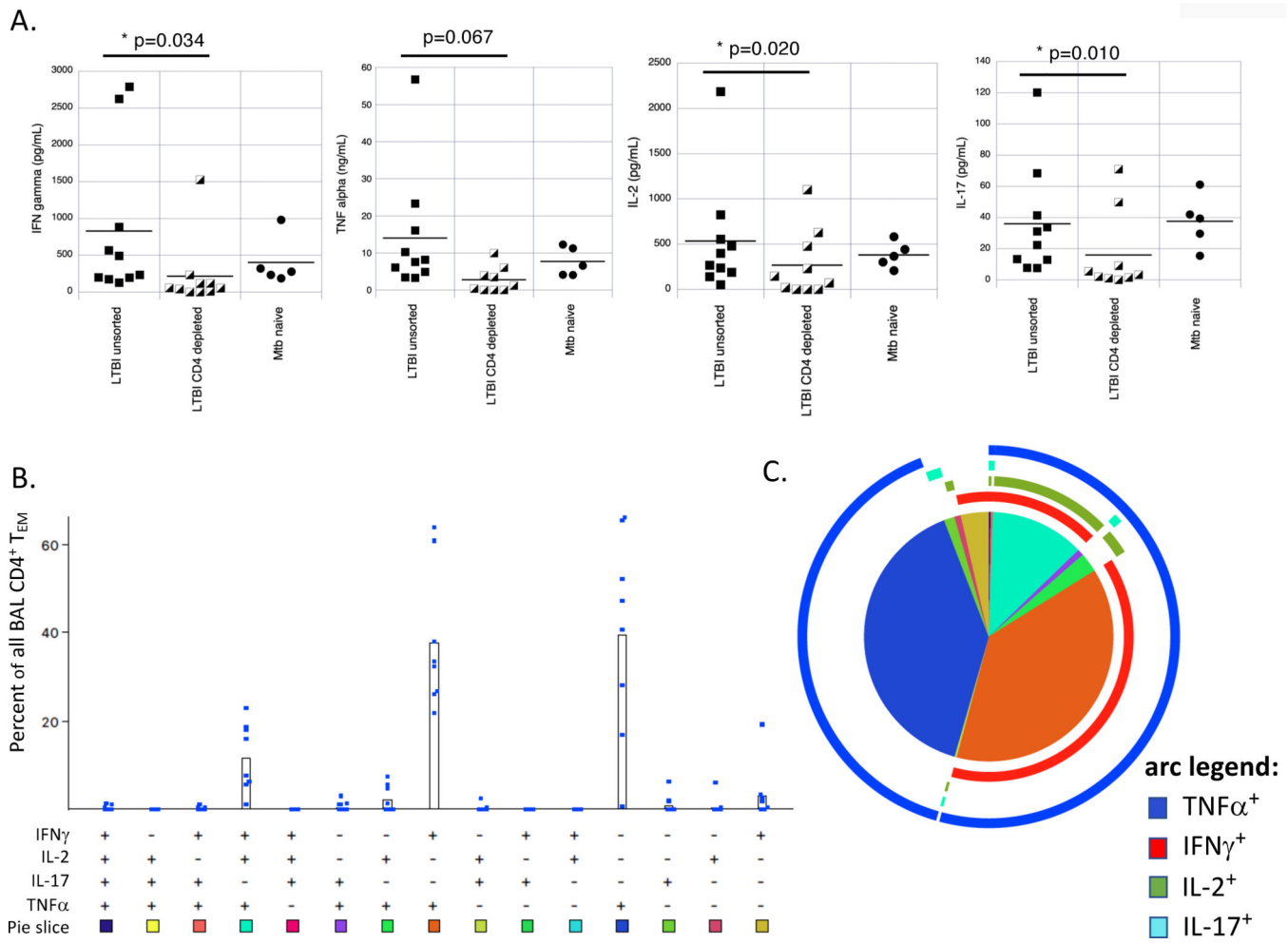

Figure 7.

Mtb-responsive resident airway CD4+ T-cells of LTBI individuals produce multiple cytokines. Supernatants of *Mtb*-infected BAL cells from cultures used in our gene expression studies were evaluated for production of IFNγ, TNFα, IL-2 and IL-17. As illustrated in Figure 7A, levels of IFNγ, IL-2, and IL-17 were all significantly reduced in cultures of BAL cells from which CD4+ T cells were depleted as compared to those of unsorted BAL cells (based on paired t-tests); reduction in TNFα was observed as well but was not statistically significant. In contrast, depletion of CD8+ T cells had no significant impact on production on any of these cytokines by BAL cell of LTBI subjects (not shown). In all figures, results are represented as cytokine levels for *Mtb*-infected cultures subtracted from cultures of uninfected, unsorted BAL cells from the same individual. Cytokine levels are reported as pg/mL of culture supernatants, with the exception of TNFα, which is reported as ng/mL. Based on these findings, we also examined polyfunctionality of BAL CD4+ T_{EM} from LTBI subjects using intracellular cytokine staining for these same four cytokines in response *in vitro* stimulation with PPD. Figure 7B shows the percentage of effector-memory (CD45RA-/CCR7-) CD4+ T cells (T_{EM}) in each subject's samples that produced each of the possible 15 cytokine combinations in response to PPD. As illustrated, the most commonly observed PPD-induced cytokine profiles were single production of

TNFα and dual production of TNFα and IFNγ, with polyfunctional production of TNFα, IFNγ and IL-2 being the next most common. These findings are represented in pie chart form in Figure 7C. The very low number of CD4+ T_{EM} producing all 4 cytokines are indicated by the thin black slice pointing straight upward; from there, the remaining combinations of three, two and single cytokines proceed clockwise in the same order displayed in 7B. The colored arcs indicate production of each of the measured cytokines. As indicated, TNFα (dark blue arc) is the most frequently observed cytokine produced by PPD-responsive BAL CD4+ T_{EM}, followed by IFNγ (red arc), IL-2 (green arc), and IL-17 (light blue arc).

Table I:

BAL cell parameters in LTBI and *Mtb*-naïve subjects

parameter	LTBI	*Mtb* naive	p-value
BAL cell count	1.38e7 (+/− 6.29e6)	1.82e7 (+/−7.45e6)	0.2221
Differential counts (%)			
macrophages	91.14 (+/− 11.03)	92.75 (+/− 3.91)	0.7354
lymphocytes	2.99 (+/− 2.51)	4.78 (+/− 2.75)	0.1788
neutrophils	5.71 (+/− 11.44)	2.25 (+/− 2.07)	0.4780
eosinophils	0.15 (+/− 0.22)	0.22 (+/− 0.40)	0.6336
CD4:CD8 ratio	3.14 (+/−1.43)	3.38 (+/− 1.58)	0.7372

BAL parameters of samples from LTBI and *Mtb*-naïve subjects used in microarray assessments of gene expression. As noted, no significant differences were observed between the two groups with regard to total or differential cell counts, or to BAL CD4:CD8 ratios. P-values were determined from non-paired t-tests as assessed with Prism software.

Table II:

Canonical pathways associated with *Mtb*-induced BAL cell gene expression in LTBI subjects

Canonical pathways with -log p-value >3.0 (from *Mtb*-induced gene expression in LTBI subjects)	LTBI unsorted	LTBI CD4 depleted	Δ-log p
Interferon Signaling	**10.666**	**0.342**	**10.323**
Crosstalk between Dendritic Cells and Natural Killer Cells	**10.347**	**1.987**	**8.360**
Pathogenesis of Multiple Sclerosis	**6.057**	**0.000**	**6.057**
Th1 Pathway	**7.473**	**1.781**	**5.692**
Antigen Presentation Pathway	**5.277**	**0.000**	**5.277**
Type I Diabetes Mellitus Signaling	**6.294**	**1.102**	**5.192**
Activation of IRF by Cytosolic Pattern Recognition Receptors	**5.127**	**0.210**	**4.917**
CD40 Signaling	**5.694**	**0.862**	**4.833**
Role of Pattern Recognition Receptors in Recognition of Bacteria and Viruses	**8.772**	**4.212**	**4.560**
Role of Hypercytokinemia/hyperchemokinemia in the Pathogenesis of Influenza	**6.694**	**2.446**	**4.249**
Th1 and Th2 Activation Pathway	**6.791**	**2.614**	**4.178**
JAK/Stat Signaling	**5.367**	**1.301**	**4.066**
IL-15 Production	**4.465**	**0.437**	**4.027**
Altered T Cell and B Cell Signaling in Rheumatoid Arthritis	**7.441**	**3.493**	**3.948**
iNOS Signaling	**4.194**	**0.288**	**3.906**
Primary Immunodeficiency Signaling	**4.636**	**0.898**	**3.737**
Role of JAK1, JAK2 and TYK2 in Interferon Signaling	**3.658**	**0.000**	**3.658**
Dendritic Cell Maturation	**6.869**	**3.235**	**3.634**
Toll-like Receptor Signaling	**5.061**	**1.473**	**3.588**
Graft-versus-Host Disease Signaling	**7.030**	**3.571**	**3.460**
Communication between Innate and Adaptive Immune Cells	**9.139**	**5.680**	**3.458**
Atherosclerosis Signaling	**6.668**	**3.682**	**2.986**
IL-10 Signaling	**4.541**	**1.592**	**2.949**
Allograft Rejection Signaling	**3.868**	**0.959**	**2.909**
Hepatic Fibrosis / Hepatic Stellate Cell Activation	**5.784**	**3.025**	**2.760**
Role of MAPK Signaling in the Pathogenesis of Influenza	**3.640**	**0.966**	**2.674**
NF-κB Signaling	**3.597**	**1.163**	**2.434**
Agranulocyte Adhesion and Diapedesis	**5.524**	**3.255**	**2.269**
Acute Phase Response Signaling	**4.938**	**2.700**	**2.237**
T Helper Cell Differentiation	**3.871**	**1.657**	**2.214**
Oncostatin M Signaling	**3.868**	**1.727**	**2.142**
IL-6 Signaling	**4.964**	**2.881**	**2.084**
Autoimmune Thyroid Disease Signaling	**3.050**	**1.003**	**2.047**
HMGB1 Signaling	**4.818**	**2.795**	**2.023**
IL-17A Signaling in Airway Cells	3.350	1.418	1.932
Th2 Pathway	3.930	2.071	1.859

Canonical pathways with -log p-value >3.0 (from *Mtb*-induced gene expression in LTBI subjects)	**LTBI unsorted**	**LTBI CD4 depleted**	**Δ-log p**
Granulocyte Adhesion and Diapedesis	8.079	6.339	1.739
Antioxidant Action of Vitamin C	3.290	1.635	1.655
Differential Regulation of Cytokine Production in Intestinal Epithelial Cells by IL-17A and IL-17F	3.751	2.197	1.554
IL-15 Signaling	3.350	2.056	1.294
MIF-mediated Glucocorticoid Regulation	3.115	1.835	1.280
Colorectal Cancer Metastasis Signaling	3.135	2.118	1.017
LXR/RXR Activation	3.221	2.397	0.824
Role of Macrophages, Fibroblasts and Endothelial Cells in Rheumatoid Arthritis	3.980	3.296	0.685
Role of IL-17A in Arthritis	3.730	3.060	0.669
TREM1 Signaling	5.229	4.678	0.551
Inhibition of Matrix Metalloproteases	4.556	4.443	0.113
Hepatic Cholestasis	4.021	4.200	-0.179
Differential Regulation of Cytokine Production in Macrophages and T Helper Cells by IL-17A and IL-17F	3.126	3.715	-0.588
Role of Cytokines in Mediating Communication between Immune Cells	3.821	4.802	-0.981
Role of IL-17F in Allergic Inflammatory Airway Diseases	3.405	5.335	-1.929

Canonical pathways associated with *Mtb*-induced gene expression in LTBI subjects. Pathway analysis was based on IPA assessment of genes identified as having significant changes in expression following *in vitro* infection of unsorted BAL cells from individuals with LTBI, and from BAL cells from which CD4+ T cells were depleted prior to *Mtb* infection. Pathways are ordered by the differences in the degree to which they were identified as significant in assessments of unsorted and CD4-depleted BAL cells (as indicated by Δ -log p-value). Of the 51 pathways identified in unsorted BAL cells by the p-value cut-off of <0.001 (-log p > 3.0), 34 (shown in **bold**) displayed a reduction in significance of > 2 logs following CD4 depletion.

J Immunol. Author manuscript; available in PMC 2020 October 15.

Table III:

Mtb-induced gene expression signature in baseline bronchoalveolar lavage cells from individuals with LTBI

						Δ – log (p-value)	
				-log (p-value)		LTBI unsorted vs LTBI CD4 depleted	LTBI unsorted vs. *Mtb*-naïve unsorted
Symbol	**Entrez Gene Name**	**ID**	**LTBI unsorted**	**LTBI CD4 depleted**	***Mtb*-naïve unsorted**		
CXCL9	C-X-C motif chemokine ligand 9	8101118	9.239	0.032	0.138	9.206	9.100
CD40	CD40 molecule	8063156	9.221	0.032	2.846	9.189	6.375
IFI35	interferon induced protein 35	8007446	8.490	0.032	0.138	8.458	8.352
TAP2	transporter 2, ATP binding cassette subfamily B member	8178841	7.097	0.032	0.138	7.065	6.959
CXCL10	C-X-C motif chemokine ligand 10	8101126	6.929	0.032	0.138	6.897	6.791
UBD	ubiquitin D	8124650	6.929	0.032	0.138	6.897	6.791
CXCL11	C-X-C motif chemokine ligand 11	8101131	6.612	0.032	0.138	6.580	6.474
TAP1	transporter 1, ATP binding cassette subfamily B member	8180061	5.917	0.032	2.077	5.885	3.840
IL15RA	interleukin 15 receptor subunit alpha	7931899	7.370	1.771	5.278	5.599	2.092
JAK2	Janus kinase 2	8154178	5.305	0.032	0.138	5.273	5.167
FAS	Fas cell surface death receptor	7929032	4.753	0.032	0.138	4.721	4.615
PNPLA3	patatin like phospholipase domain containing 3	8073633	4.690	0.032	0.138	4.658	4.552
CCL5	C-C motif chemokine ligand 5	8014316	4.690	0.032	2.135	4.658	2.555
PARP9	poly(ADP-ribose) polymerase family member 9	8090018	4.614	0.032	0.138	4.582	4.476
IFNG	interferon gamma	7964787	4.593	0.032	0.138	4.561	4.455
PSMB9	proteasome subunit beta 9	8118571	4.519	0.032	0.138	4.487	4.381
CD274	CD274 molecule	8154233	4.497	0.032	0.138	4.465	4.359
PSME2	proteasome activator subunit 2	7978123	4.050	0.032	0.138	4.018	3.912
MX1	MX dynamin like GTPase 1	8068713	3.861	0.032	0.138	3.829	3.723
IL10RA	interleukin 10 receptor subunit alpha	7944152	3.777	0.032	0.138	3.745	3.639
RARRES3	retinoic acid receptor responder 3	7940775	3.546	0.032	0.138	3.514	3.408
LTA	lymphotoxin alpha	8118137	3.441	0.032	0.138	3.409	3.303
PARP14	poly(ADP-ribose) polymerase family member 14	8082100	3.411	0.032	0.138	3.379	3.273
RFX5	regulatory factor X5	7919971	3.411	0.032	0.138	3.379	3.273

						Δ – log (p-value)	
				-log (p-value)		LTBI unsorted vs LTBI CD4 depleted	LTBI unsorted vs. *Mtb*-naïve unsorted
Symbol	**Entrez Gene Name**	**ID**	**LTBI unsorted**	**LTBI CD4 depleted**	***Mtb*-naïve unsorted**		
IFIT3	interferon induced protein with tetratricopeptide repeats 3	7929052	3.044	0.032	0.138	3.012	2.906
IL15	interleukin 15	8097553	3.000	0.032	0.138	2.968	2.862
IL27	interleukin 27	8000567	3.000	0.032	0.138	2.968	2.862
NECTIN2	nectin cell adhesion molecule 2	8029507	3.000	0.032	0.138	2.968	2.862
IRF1	interferon regulatory factor 1	8114010	2.975	0.032	0.138	2.943	2.836
TNFSF10	TNF superfamily member 10	8092169	2.970	0.032	0.138	2.938	2.832
KL	klotho	7968556	2.899	0.032	0.138	2.867	2.761
IFITM3	interferon induced transmembrane protein 3	7945371	2.890	0.032	0.138	2.858	2.752
STAT2	signal transducer and activator of transcription 2	7964119	2.890	0.032	0.138	2.858	2.752
CSF2RB	colony stimulating factor 2 receptor beta common subunit	8072757	2.853	0.032	0.138	2.821	2.714
HLA-F	major histocompatibility complex, class I, F	8179019	2.753	0.032	0.138	2.721	2.615
PSMB8	proteasome subunit beta 8	8125500	2.734	0.032	0.138	2.702	2.596
CD226	CD226 molecule	8023757	2.641	0.032	0.138	2.609	2.503
MAP2K1	mitogen-activated protein kinase kinase 1	7984319	2.598	0.032	0.138	2.566	2.460
GZMB	granzyme B	7978366	3.887	1.377	1.657	2.510	2.230
PSME1	proteasome activator subunit 1	7973564	2.390	0.032	0.138	2.358	2.252
ICOS	inducible T cell costimulator	8047702	2.388	0.032	0.138	2.356	2.250
AICDA	activation induced cytidine deaminase	7960910	2.372	0.032	0.138	2.340	2.234
USP53	ubiquitin specific peptidase 53	8097098	2.231	0.032	0.138	2.199	2.093
DNAJC7	DnaJ heat shock protein family (Hsp40) member C7	8015490	2.217	0.032	0.138	2.185	2.079
NLRC5	NLR family CARD domain containing 5	7995926	2.199	0.032	0.138	2.167	2.061
SOCS2	suppressor of cytokine signaling 2	7957551	2.177	0.032	0.138	2.145	2.039
CD80	CD80 molecule	8089771	2.146	0.032	0.138	2.114	2.008

Set of 47 genes identified as the signature of the impact of memory CD4+ T cells on *Mtb*-induced BAL cell gene expression. As detailed in the text, delineation of this gene signature was derived from evaluation of 12 canonical pathways identified with a probability of $p<0.001$ in unsorted BAL cells from LTBI subjects, and with a reduction in significance of at least 2 logs in both CD4+ T-cell depleted LTBI samples and BAL cells from *Mtb* naïve subjects (illustrated in Figure 2B). Of 68 differentially-expressed genes within these 12 pathways, the expression of the 47 genes of this signature in unsorted BAL cells of LTBI subjects also met criteria of p-value significance 2 logs greater than observed in both CD4-depleted BAL samples from LTBI subjects and unsorted BAL cells from *Mtb*-naïve subjects, as displayed in the two furthest right columns of Table III.

Table IV:

Top 20 upstream regulators not associated with Type I IFN, as based on impact of T-cell depletion on –log (adjusted p-values)

CD4 top upstream regulators			CD8 top upstream regulators	
Regulator	***Change in –(log p) with CD4 depletion***		***Regulator***	***Change in –(log p) with CD8 depletion***
IFNG	40.37		**TNF**	11.03
LPS	35.31		**IL27**	7.98
Poly I:C RNA	34.72		IL10RA	5.69
CD40LG	28.06		NKX2	5.47
TNF	24.27		CpG nucleotide	5.30
TLR4	23.69		**IFNG**	5.28
STAT3	23.07		CREBBP	5.12
TLR3	21.19		NLRC5	5.02
TICAM	21.04		fluticasone	4.92
CD40	20.32		IL6	4.88
IL27	20.03		IL27RA	4.78
TLR9	19.49		PARP1	4.54
TLR7	19.21		MAPK1	3.90
STAT6	17.74		Mir-21	3.86
TRIM24	17.71		IL1RN	3.84
IL10	17.38		SOCS1	3.74
IL1B	17.12		STAT5A	3.67
TCR	16.94		GATA2	3.11
BTK	16.75		SMARCA4	3.07
NIKX2–3	16.35		KIT	2.97

Top 20 *Mtb*-induced upstream regulators of BAL cell gene expression not associated with Type I interferons. Results are expressed in terms of the decrease in significance (-log p-value) following depletion of CD4+ or CD8+ T cells. As shown, with the exceptions of IFNγ, TNFα, and IL-27 (indicated in **bold**) the lists do not overlap; further, the reductions in significance of the various regulations is far greater following depletion of CD4+ as compared to CD8+ T-cells.